$\mathcal{K}$ $\mathcal{D}$

# DEVELOPMENT OF AN OPTICAL DISC RECORDER

## FINAL TECHNICAL REPORT

Sponsored by

### DEFENSE ADVANCED RESEARCH PROJECTS AGENCY

DARPA Order No. 3080
Program Code No. 6D30

Contract No. N00014-76-C-0441

Principal Investigator:   George Kenney   (914) 762-0300
Scientific Officer:   Marvin Denicoff

Amount of Contract:   $774,900
Contract Period:   1 Oct. 1975 - 1 Oct. 1977

THE VIEWS AND CONCLUSIONS CONTAINED IN THIS DOCUMENT
ARE THOSE OF THE AUTHORS AND SHOULD NOT BE INTERPRETED
AS NECESSARILY REPRESENTING THE OFFICIAL POLICIES,
EITHER EXPRESSED OR IMPLIED, OF THE ADVANCED RESEARCH
PROJECTS AGENCY OR THE U.S. GOVERNMENT.

D D C
RECEIVED
MAR 6 1978
A

Prepared by

## PHILIPS LABORATORIES

A Division of North American Philips Corporation
Briarcliff Manor, New York 10510

January 1978

| REPORT DOCUMENTATION PAGE | | READ INSTRUCTIONS BEFORE COMPLETING FORM |
|---|---|---|
| 1. REPORT NUMBER | 2. GOVT ACCESSION NO. | 3. RECIPIENT'S CATALOG NUMBER |
| 4. TITLE (and Subtitle)<br><br>DEVELOPMENT OF AN OPTICAL DISC RECORDER | | 5. TYPE OF REPORT & PERIOD COVERED<br>Final Technical Report<br>1 Oct. 1975 - 1 Oct. 1977<br>6. PERFORMING ORG. REPORT NUMBER |
| 7. AUTHOR(s)<br>George<br>G./Kenney, D./Lou, J./Wagner, F./Zernike<br>R./McFarlane, A. Milch, A. Chan | | 8. CONTRACT OR GRANT NUMBER(s)<br>N00014-76-C-0441,<br>DARPA Order-0380 |
| 9. PERFORMING ORGANIZATION NAME AND ADDRESS<br>PHILIPS LABORATORIES<br>A Division of North American Philips Corp.<br>Briarcliff Manor, New York 10510 | | 10. PROGRAM ELEMENT, PROJECT, TASK AREA & WORK UNIT NUMBERS<br>DARPA Order No. 0380<br>Program Code No. 6D30 |
| 11. CONTROLLING OFFICE NAME AND ADDRESS<br>Defense Advanced Research Projects Agency<br>1400 Wilson Boulevard<br>Arlington, Virginia 22209 | | 12. REPORT DATE<br>January 1978<br>13. NUMBER OF PAGES<br>101   101 p. |
| 14. MONITORING AGENCY NAME & ADDRESS(if different from Controlling Office)<br>Office of Naval Research<br>800 North Quincy Street<br>Arlington, Virginia 22217<br>Code: 437 | | 15. SECURITY CLASS. (of this report)<br>UNCLASSIFIED<br>15a. DECLASSIFICATION/DOWNGRADING SCHEDULE |

16. DISTRIBUTION STATEMENT (of this Report)

Approved for public release:  Distribution unlimited.

D D C

MAR 6 1978

A

17. DISTRIBUTION STATEMENT (of the abstract entered in Block 20, if different from Report)

18. SUPPLEMENTARY NOTES

19. KEY WORDS (Continue on reverse side if necessary and identify by block number)

| | |
|---|---|
| optical disc recorder | disc protective mechanism |
| direct-read-after-write | disc |
| lasers | sled |
| substrate materials | air sandwich |
| recording materials | |

20. ABSTRACT (Continue on reverse side if necessary and identify by block number)

A laboratory-prototype, digital, optical disc recorder was developed with a storage capacity of $10^{10}$ bits.  Recording is done by laser machining of micron-sized pits in a thin tellurium film allowing direct-read-after-write (DRAW) of the information. The recording format maps each bit of information to a recorded pit.  The tellurium is deposited on a clear plastic disc configured to be self-protecting and easily handled. The major accomplishment was demonstrating the feasibility of an inexpensive recorder and disc suitable for operation in a normal office environment.  The key developments were a sensitive recording material, a plastic disc, and a self-protected disc configuration called the "air sandwich".  All of the design goals were met.

DD FORM 1473  EDITION OF 1 NOV 65 IS OBSOLETE
1 JAN 73

387  334   JOB

# SUMMARY

*10 to the 10th power*

A laboratory-prototype, digital, optical disc recorder was developed with a storage capacity of $10^{10}$ bits. Recording is done by laser machining of micron-sized pits in a thin tellurium film allowing (direct-read-after-write (DRAW) of the information. The recording format maps each bit of information to a recorded pit. The tellurium is deposited on a clear plastic disc configured to be self-protecting and easily handled.

The major accomplishment was demonstrating the feasibility of an inexpensive recorder and disc suitable for operation in a normal office environment. The key developments were a sensitive recording material, a plastic disc, and a self-protected disc configuration called the "air sandwich".

Various materials were considered for the disc substrate and its protection; selection was based primarily on macro and microscopic flatness, thickness uniformity, strength, optical properties, adherence of DRAW film, and cost. Polymethylmethacrylate (trade name, Lucite, Plexiglas, Perspex) was selected as the primary disc material. The choice of tellurium as the recording material allows direct monitoring of the recording quality; no development or fixing of the recording is necessary. The air-sandwich configuration localizes the "clean room" requirement to the disc itself, thereby eliminating the special handling precautions and environment that an unprotected master record would require.

All of the design goals were met, viz.:

- Design, fabrication, and test of a prototype DRAW recorder.

- Selection of a suitable disc substrate (Plexiglas).

- Design and test of a disc protective mechanism (air sandwich).

- Demonstration of two suitable DRAW materials (tellurium and bismuth).

- Shelf-life characterization of tellurium and bismuth.

- Demonstration of a working error-detection and correction system.

- System concept amenable to a disc cost of < $10 and a recorder cost of < $10,000 in production quantities.

# TABLE OF CONTENTS

## TABLE OF CONTENTS (Cont'd.)

# LIST OF ILLUSTRATIONS

## LIST OF ILLUSTRATIONS (Cont'd)

9

# 1. INTRODUCTION

## 1.1 General

The objective of this program was to develop a laboratory-prototype, digital, optical disc recorder with the following characteristics as design goals:

- Direct read after write (DRAW) capability
- No processing of recording materials required
- Storage capacity > $10^{10}$ bits
- Corrected error rate of $10^{-9}$
- 1 $\mu m$ minimum bit size
- 2 $\mu m$ track-to-track spacing
- 40,000 tracks of $4.4 \times 10^5$ bits each
- Average track time of 600 ms
- 1.33 Mbit data rate
- Discs cost < \$10 in quantity
- Recorder manufacturable for \$5,000 to \$10,000

The major task was to demonstrate the feasibility of an inexpensive recorder suitable for operation in a normal office environment. A sensitive recording material and a self-protected plastic disc were key developments necessary to achieve these goals.

The optical recorder program was based on technology developed by N.V. Philips, Eindhoven, the Netherlands, for a videodisc system designed for home entertainment. In that videodisc system, recording is done in photoresist that is coated on a polished glass master; the photoresist is then developed after recording. These master discs are heavy, expensive, and require a clean-room recording environment for protection. Further, the home entertainment system was designed to take advantage of an inexpensive replication process in order to minimize the cost of the record.

In the current application, there were different constraints. In particular, no processing of the disc was allowed, thereby

11

requiring an immediate, "self-developing" type of recording. This requirement was satisfied by laser-forming pits in a thin metallic film; the recorded pit (information) can then be read directly after writing (DRAW). Tellurium and bismuth were found to be acceptable DRAW films.

Another major requirement was the replacement of the polished glass masters used in the home entertainment system. A considerable portion of the program effort was devoted to developing an inexpensive, self-protected, master-quality disc. Various materials were considered for the disc substrate and its protection; selection was based primarily on macro and microscopic flatness, thickness uniformity, strength, optical properties, adherence of DRAW films, and cost. Polymethylmethacrylate (trade names, Lucite, Plexiglas, Perspex) was selected as the primary disc material.

After the program was underway, it was recognized that the general utility of the recording system would be significantly affected by the storage life of the recording material on which the system was based. A new task was added by contract modification to study and evaluate the factors affecting the degradation of materials considered suitable for optical recording and to establish preliminary indications of the storage life.

## 1.2 Background

Since the technology for the DRAW system program was, in part, based on the Philips/MCA consumer videodisc system (Fig. 1), a brief introduction to this system is presented.

The system (Fig. 2) has a rotating glass master disc and a modulated laser beam. The light beam is focused to a micron-size spot on the surface of the master disc. The disc's surface, which is coated with a photoresist layer, is exposed to the modulated and focused laser beam. The light is modulated by an electrical signal composed of video and audio information.

Figure 1:   Philips/MCA videodisc system.
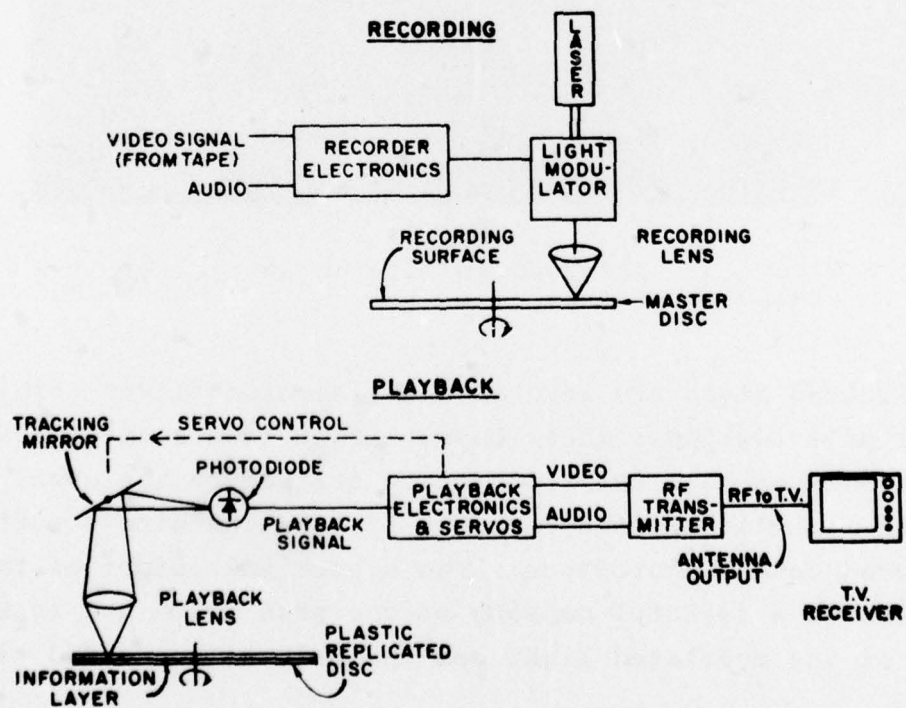


Figure 2:   Recording and playback process of videodisc system.

13

After development of the photoresist, the result is a recording of pits which maps the light modulation.

Following a procedure similar to that used to produce audio long playing records, a nickel stamper copy is prepared from the master disc. Plastic discs are then replicated from the stamper. Figure 3 shows the information pits on the surface of a replicated videodisc. The plastic discs are coated with a reflective aluminum layer to facilitate optical readback.



Figure 3: Information pits on surface of videodisc system.

The replicated discs are read on the videodisc player (Fig. 1) by means of a low-power laser beam. Light from a small HeNe laser is focused onto the information surface on the disc. The reflected light is modulated by the pits on the disc's surface and focused onto a photodiode. The electrical output of the photodiode is a faithful mapping of the pits which are in turn a mapping of the modulated light and the original recorded signal.

After appropriate processing, the playback signal is ready for display on a normal television set. There are 54,000 tracks, each containing a full color picture. The normal playing time is 30 minutes of video and audio information. A more complete description of the consumer videodisc system is given by Bogels (Ref.1).

## 2. DESIGN APPROACH

The system concept was based on using an inexpensive HeNe laser to machine pits in a thin film of highly absorbent material. Maydan (Ref. 2) demonstrated the feasibility of forming 6 $\mu$m holes in thin bismuth films. Subsequent work by Precision Instruments (Ref. 3), MCA (Ref. 4), and N.V. Philips, demonstrated recording of information in thin metallic films. Tellurium and bismuth films were selected for study.

Tellurium was chosen as the most attractive recording medium based on the requirements for sensitivity, resolution, reproducibility and archival storage. Bismuth was also found to be an acceptable DRAW material; although not as sensitive as tellurium, bismuth is considered an acceptable, back-up recording film. The sensitivity of either material is sufficient to allow at least 2 Mbit/s recording with a 25 mW HeNe laser.

The shelf-life properties of tellurium and bismuth films were investigated (see Appendix A). The reflection, transmission and hole machining properties were measured in a high-temperature, accelerated life test. The films were found to be stable at all temperatures for the entire test. While there are some reservations about the validity of temperature stress aging, the approach is an attractive alternative to real-time testing. Only an indication of shelf life can be extracted from accelerated aging tests. However, if one assumes an activated process such as oxidation, the test results indicate a shelf life of ten years at room temperature.

Some means for protecting the recording, other than a clean room facility, was required. The tellurium film must be protected from scratches, dust, and fingerprints before, during, and after recording. All the techniques considered were directed at self-protecting the disc by means of a transparent cover. According to Bogels (Ref. 1), a 400 $\mu$m protective separation from the information sufficiently defocuses any surface imperfections. Therefore, a conservative cover thickness of 1 mm was chosen.

16

A disc protective mechanism called the air sandwich was developed, which has the following advantages: protection of the recording layer without degrading recording sensitivity, containment of vapors or other products produced during recording, and a two-sided configuration. The air sandwich consists of two discs, each coated with a tellurium layer and separated by ring gaskets at the inner and outer radii of the information band. The annular cavity between the two discs is essentially a miniature clean room which protects the tellurium layer before, during, and after recording.

The optical and mechanical properties of the air sandwich disc are comparable to those of the consumer videodisc. In fact, air sandwich discs were played on a modified consumer videodisc player. A manufacturing cost of $10. per air sandwich disc is anticipated.

The first recorder (Fig. 4) used for the investigations at Philips Laboratories (PL) was similar to the mastering recorder of N.V. Philips (NVP). It was designed and built at NVP for use with polished glass masters, but was modified at PL to allow recording on PMMA discs. A blue argon laser was used for recording; a second low-powered HeNe laser was used for playback. The NVP recorder served for many routine experiments in materials and disc evaluation; however it was never intended to fulfill the needs of the program.

In addition to modifying the NVP recorder for use as a test vehicle, the program included a study of the various subsystems of an optical disc recorder. New designs for the mechanical, optical, and electrical subsystems were fabricated and tested. The result of this effort was a new DRAW recorder laboratory prototype (Fig. 5).

The prototype design was greatly influenced by the program objective to demonstrate the feasibility of an inexpensive recorder. The argon ion laser and wide-band, electro-optic

17
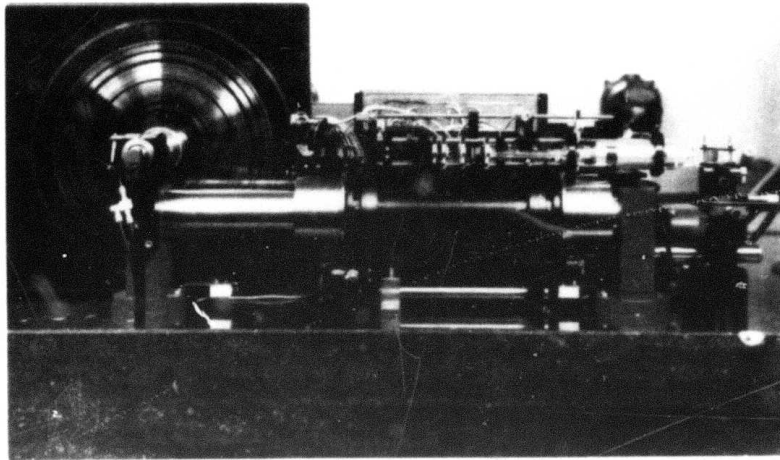
Figure 4: N.V. Philips DRAW optical system installed at Philips Laboratories.
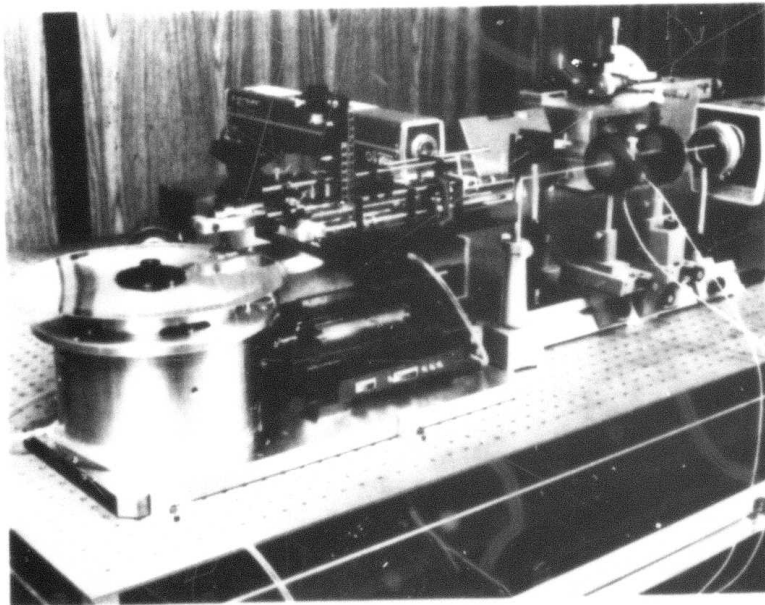


Figure 5: Assembled Philips Laboratories prototype DRAW optical recorder.

modulator used on the NVP master recorder are expensive. Therefore, a 25 mW HeNe laser and a low bandwidth acousto-optic modulator were chosen on the basis of potential low cost and reliability.

Additionally, the prototype DRAW recorder differed from the NVP recorder in the disc orientation, turntable and sled configuration, and optical system. The disc rotates on a vertical axis. The turntable is air-bearing-supported, which provides radial stability of the axis of rotation. The disc speed is servo controlled. The optical sled of the recorder travels on a rectangular cross-section air-bearing. The sled is driven along a radius of the disc by a linear electric motor. The sled velocity is measured by a velocity transducer and is servo controlled. The combination of a light, air-bearing sled and a linear motor offered an attractive solution to the twin problems of uniform, ultra-slow, radial motion required for recording and reasonably fast access of information required during playback. Although a random access system was never built, the prototype sled is capable of an average access time of 500 ms.

Focusing and tracking systems similar to those of the consumer videodisc system (Ref. 1) were used to correct for the radial and flatness irregularities of the air sandwich disc. The optical system uses a single laser with the beam split into two spots, one for recording and one for playback. The playback spot trails the recording spot by a few microns. In this manner, the recorded pit is read directly after writing (DRAW). The feature is necessary for high-quality, error-free digital recording.

Pseudo-random data was recorded on a tellurium, air sandwich disc. A block of $0.6 \times 10^8$ bits was successfully retrieved without error. The system first encodes the data with a triple-error correcting convolutional code, then interleaves the data to a length of 256 bits, followed by frequency (Miller) modulation before recording on the disc. The playback signal is

processed and amplified, then demodulated using a phase-lock loop circuit. The recovered data is then decoded by the convolutional decoder. The system theoretically is capable of retrieving error-free data through disc defects as large as 1.0 mm. The encoded data rate was 1 Mbit/s; the disc rotation speed was 4 rps. According to the manufacturer, the convolutional encoder/decoder is capable of achieving error rates less than $10^{-9}$.

With a track pitch of 2 $\mu$m and an 8 cm recording band, there are 40,000 tracks on each side of the air sandwich disc. The storage capacity per disc side is $1.86 \times 10^{10}$ bits unformatted and $1.05 \times 10^{10}$ bits formatted.

In summary, all of the design goals were met by accomplishment of the following tasks:

- Design, fabrication, and test of a prototype DRAW recorder.
- Selection of a suitable disc substrate (Plexiglas).
- Design and test of a disc protective mechanism (air sandwich).
- Demonstration of two suitable DRAW materials (tellurium and bismuth).
- Shelf-life characterization of tellurium and bismuth.
- Demonstration of a working error-detection and correction system.
- System concept amenable to a disc cost of <$10 and a recorder cost of <$10,000 in production quantities.

20

## 3.    DRAW RECORDER

### 3.1    Turntable

The turntable of the DRAW recorder spins the disc on a vertical
axis.   The table consists of an air-bearing (Professional
Instrument Company, Model 4B "Blockhead") coupled directly to a
small electric motor (PMI Model OP-00909-272, Type U9M4/SPD).
The ball bearings of the motor were removed and the motor shaft
coupled concentrically to the rotor of the air bearing.   An
optical tachometer is integral to the motor.   With the inertia
of the rather heavy air bearing, it was found that the large
number of spokes (2000) on the tachometer was not needed.

The rotational velocity of the turntable is stabilized to a
master oscillator using the circuit shown in Par. 9.3.   To
determine the stability of the rotational velocity, 2000 pulses
per revolution were recorded on a disc.   This resulted in radial
spokes on the disc, each consisting of a series of pits spaced
by one track.   By measuring the deviation from straightness of
these spokes, the rotation time of 250 ms was found to have less
than 100 ns jitter in 1.25 ms.   The turntable and drive servos
are described in Par. 9.3.

The radial stability of the turntable was found to be better
than 0.1 $\mu$m.   This was determined by measurement with a prox-
imity gauge and by measurements made on recorded discs.   To
record and reproduce 1 $\mu$m pits accurately, the objective must
remain focused at all times to within $\pm$ 0.5 $\mu$m.   This was
verified experimentally.   Warping of the disc can cause vertical
excursions of the information surface by as much as 1 mm.
Therefore, any misfocus is optically sensed and reduced by an
active focusing system; this system is described in Par. 9.1

### 3.2    Sled

The sled travels on a rectangular air bearing (Dover Instruments
Model 400B) and is driven by a linear electric motor.   The sled

21

velocity is translated into a voltage by a magnetic pickup (Collins Model LMV-719-S22), and this voltage is compared to a standard to stabilize the velocity. The sled is driven at 8 $\mu$m/s for recording at 4 rps. By examining the diffraction pattern produced by a finished recording, it was found that the track spacing produced by the system varied less than 0.1 $\mu$m, i.e., the velocity of the sled varied less than 5%.

It should be noted that a good estimate of the uniformity of the track spacing can be obtained by visual examining the written disc. The sled and its drive servos are described in Par. 9.4

## 3.3    Optical System

A single-color DRAW optical system was designed and tested. A simplified schematic of the optical system is shown in Figure 6. The system works equally well at 588 nm (argon laser) and 633 nm (HeNe laser) wavelengths. The light output from the laser is split into two unequal beams: 90% for recording, 10% for play-back. The recording beam is encoded with the information signal by a light modulator. The playback beam passes two mirrors and a beam splitter, which are arranged so that the record and playback beams are recombined at the objective. The objective focusses the beams onto the information layer inside the air sandwich disc.

Since the playback beam is slightly skew to the (recording) optical axis, the playback spot trails the recording spot by a few microns. In this manner the recorded pit is read shortly after writing (DRAW), a feature necessary for high-quality, error-free recording. Any difference between the recorded and playback signal can be detected, and the information can be immediately re-recorded if necessary.

A radial tracking mirror follows the recorded tracks during a playback-only mode. The playback spot must follow the track within 0.1 $\mu$m. Since disc eccentricity can be as large as 50 $\mu$m,

22

AIR SANDWICH DISC

MODULATION SIGNAL

BEAM SPLITTER

LASER

MODULATOR

RECORD BEAM

90%

10%

PLAYBACK BEAM

FOCUS SYSTEM

OBJECTIVE

RADIAL TRACKING MIRROR

TURNTABLE

BEAM SPLITTER

PHOTO DIODE

DRAW PLAYBACK SIGNAL
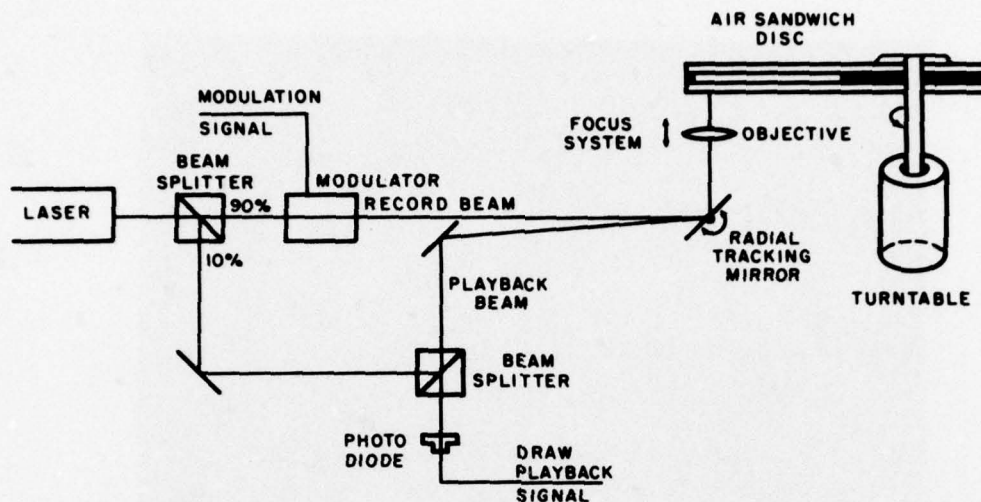
Figure 6: Simplified optical schematic of DRAW system.

the radial mirror must be controlled to reduce this error to within the 0.1 $\mu$m limits. Mistracking is optically sensed, and the error controls the radial mirror to reduce the error. The tracking servo is described in Section 9.2.

During the recording operation it is not necessary to activate the radial tracking system, and the mirror is therefore held in a fixed position. In the preliminary tests a fixed mirror was used.

With an overall light transmission through the optical system of 50%, the focused power available from a HeNe laser for recording at the disc's surface is 12 mW. Based on the sensitivity of tellurium and bismuth (Par. 4.2) for hole forming, and on the available power, the specified disc rotation speed (240 rpm) and raw data rate (1.8 Mbit/s) are conservative. Figure 7 shows a photomicrograph of pits recorded in tellurium film. The data rate was 1.8 Mbit/s at 4 rps.

23

Figure 7:  Photomicrograph of encoded pits
recorded in tellurium film.  (1300X)

## 4. DRAW MATERIAL

### 4.1 General Requirement

Consistent with the program objectives, there are basic requirements that the recording material must meet.

Resolution. To obtain the desired packing density of $10^8$ bits/$cm^2$, the material must be capable of recording micron-size bits. Proper retrieval of digital signals also requires that the bit shape be well defined to yield better than approximately 30 dB carrier-to-noise ratio on playback when measured with a 30 kHz noise bandwidth.

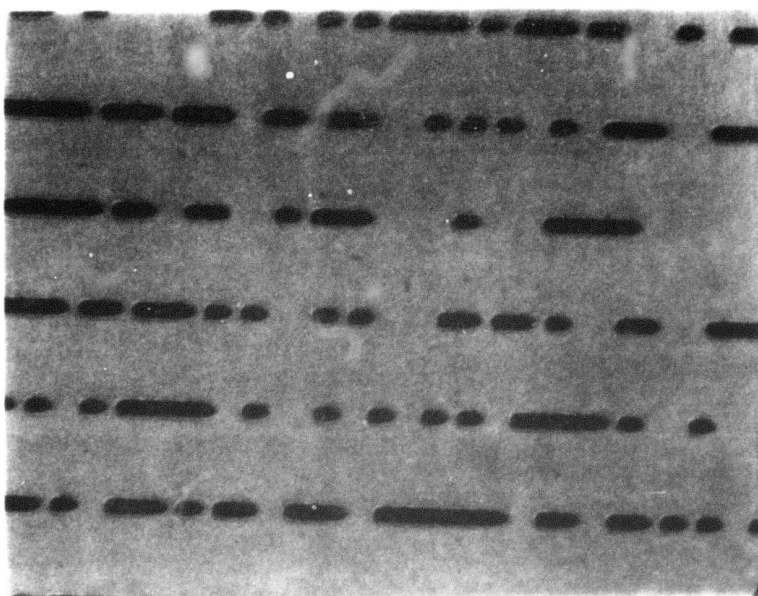Sensitivity. One can reasonably expect that a typical low-power, low-cost laser in the near future would be of the He-Cd or He-Ne variety and capable of output powers of about 20 - 25 mW. Assuming a system transmission efficiency of 40%, this implies deliverable power at the recording medium of 10 mW. To record micron-size pits at a data rate of 2 Mbits/s, the material must have a sensitivity less than 400-500 mJ/$cm^2$. A better sensitivity would allow recording at a higher data rate.

Error Rate. To achieve a retrievable error rate of $10^{-9}$, immediate verification after recording is required, i.e., the material must be DRAW (direct-read-after-write). This, therefore, precludes all optical recording material which requires a development step to define the image. The material must be capable of being deposited uniformly and be free of pin holes over a large area.

Archival Storage. The principal application of the system is expected to be in the mass storage area. It is therefore highly desirable that the recording medium has archival characteristics. Archival storage in this sense implies both shelf life, the ability to record after a given time interval, and archival life, the ability to retrieve error-free information after a time interval.

In addition, compatibility with an inexpensive recorder demands a low-cost plastic substrate and fabrication process. Further, the typical environment for mass-storage applications requires that the recording medium be protected, non-erasable, and show a definite power threshold for recording.

## 4.2    Characterization of the Laser Micromachining Process

Previous experiments published in the open literature indicate that bismuth films will probably be marginally satisfactory for meeting the requirements outlined. It was therefore decided to investigate other metal and semi-metal films, prepared by vacuum deposition on transparent plastic substrates, as recording media for the program. Preliminary experiments were carried out to study the characteristics of several metal films for laser micromachining, primarily from the point of view of identifying materials of high sensitivity in the red and near infrared wavelengths. These results are summarized in Appendix II of Reference 5.

The sensitivity, defined in terms of the laser energy per unit hole area required to form a hole of a given size, was found to depend on the substrate, film thickness, hole size, beam-spot size, and exposure duration. Thin films of tellurium, about 300 Å thick, deposited on PMMA substrates have the best sensitivity found to date. The sensitivity for machining 1 $\mu$m diameter holes with optimum beam size is in the range of 100-300 mJ/cm$^2$, depending on exposure duration.

Although the experiments were done at the argon wavelength (488 nm), the spectral properties of tellurium films were measured and reported (see Appendix B of Ref. 6). No serious degradation in performance is expected for either the He-Ne or GaAlAs laser wavelengths.

The above experiments were preliminary in the sense that the laser beam used for machining was stationary with respect to the substrate. In an actual recorder, with the disc

rotating, there would be relative motion between the laser beam and the substrate. Two different analyses were carried out to investigate the behavior of laser micromachining under dynamic conditions. An analysis, assuming an adiabatic process for laser machining, but taking into account Gaussian energy distribution in a laser beam, is reported in Appendix C of Ref. 7. This analysis shows that under the dynamic conditions anticipated in a typical recorder, the holes produced would have an oblong shape, with sharp straight boundaries parallel to the direction of motion and roughly semicircular boundaries perpendicular to the direction of motion. The optimum beam size (defined in terms of power to 1/e of maximum) required to produce a hole of width w is about $\sqrt{2}\ w$. Under the optimum condition, the power required to produce a 1 $\mu$m x 1 $\mu$m hole is slightly less than the power required under static conditions, whereas the power required for a 2 $\mu$m x 1 $\mu$m hole would be about twice the static power.

An analysis of dynamic hole machining was made which took into account the heat dissipation into the substrate, but with a beam profile which was a one-dimensional strip. The salient result of this analysis was that the temperature profile in the film arising from the absorption of laser energy can be described in terms of a function $F(\alpha,r)$. Here $\alpha$ is a parameter describing the thermal mismatch between film and substrate, and r is a dimensionless variable of the order of $\delta/\sqrt{D_f t}$, where $\delta$ = film thickness, $D_f$ = thermal diffusivity of film material and t = time scale involved in the machining process. For $r \gtrsim 1$, $F(\alpha,r)$ is independent of $\alpha$, and the machining process becomes adiabatic. The analysis showed that the process was adiabatic for exposure durations of interest.

Neither of these analyses included the effect of the film substrate interface, which probably plays an important role in the hole formation process. Initial measurements of the laser machining characteristics under dynamic conditions just prior to

27

termination of the program indicated sensitivities substantially better than that predicted by theory.

### 4.3    DRAW Recording

A semi-clean facility for fabricating tellurium air sandwiches was constructed.  The room had all the facilities necessary to produce air sandwiches, including disc cleaning, vacuum deposition and air sandwich bonding.  Many air sandwiches were assembled for experiments on DRAW recording.

Most of these experiments (described in the following paragraphs) were done on the NVP recorder, using a Lexel Model 85 argon laser and Harris Model 180 acousto-optic modulator.  The feasibility of recording and playing back a single-frequency test signal at better than 40 dB carrier-to-noise ratio was demonstrated for the tellurium air sandwich structure.  Figure 8 shows a typical playback signal; an SEM photograph of the recorded pits is shown in Figure 9.

The feasibility of recording with a He-Ne laser was demonstrated with a Spectra Physics Model 907 He-Ne laser with 25 mW output power.  Modulation was provided by the Harris Model 180 acousto-optic modulator.  Pulse exposure duration was 500 ns, given a data rate of 2 Mbits/s.  Micron-size holes were machined on 300 $\overset{\circ}{A}$ thick tellurium films deposited on polyisobutyl methacrylate-coated glass masters.  Figure 10 shows a picture of the pits taken on an optical microscope.

Measurements on the power required for recording indicate dynamic sensitivities much better than what one would expect on the basis of the discussions in Section 3.  With available laser power and film sensitivities, data rates up to 10 MBits/s seem reasonable.

Pseudo-random data was recorded on a tellurium air sandwich disc using Linkabit error-correction electronics; a block of $6 \times 10^8$

28
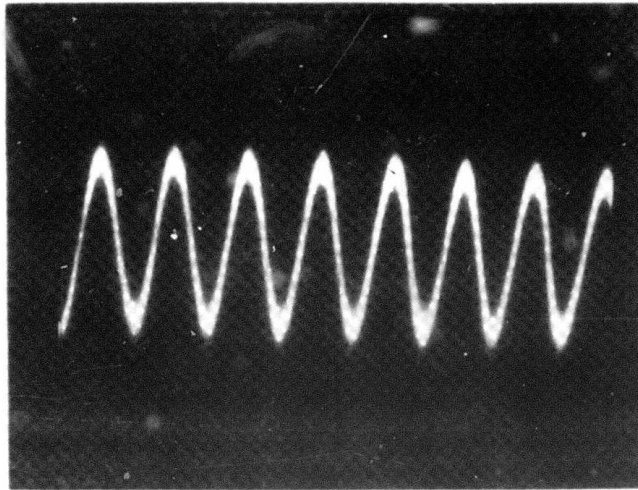
Figure 8:   Playback of signal with 40 dB SNR.
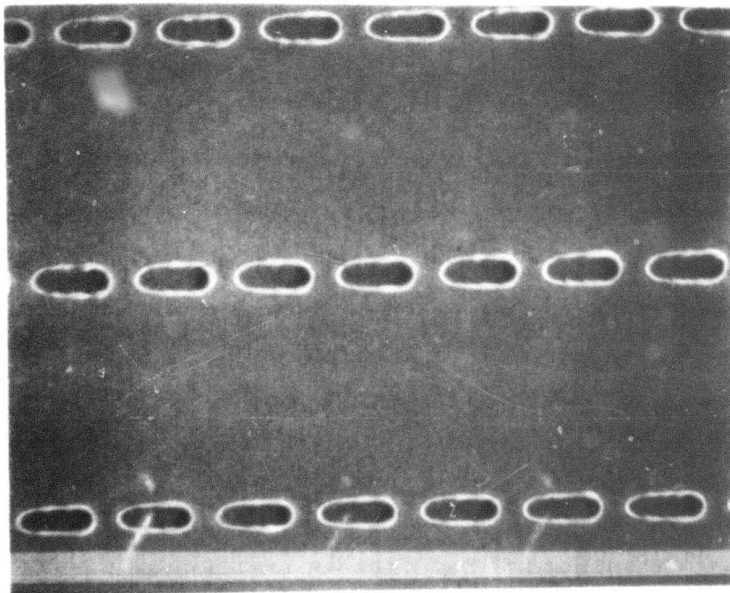


Figure 9.   SEM photograph of recorded pits.
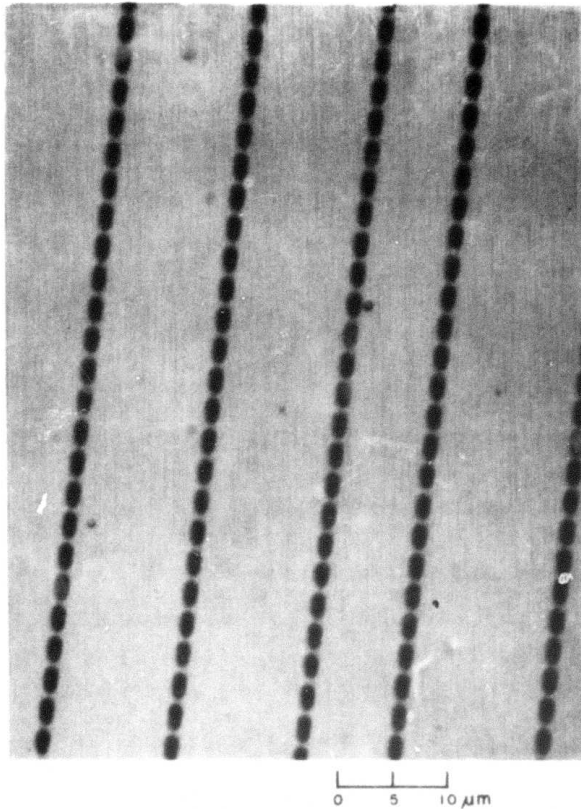
Figure 10: 25 mW HeNe laser on 300 Å Te on PMMA-coated glass master. Disc rotation speed about 400 rpm.

bits was successfully retrieved without error (see Sect.8). According to Linkabit, error rates of less than $10^{-9}$ are possible with the tellurium-disc channel characteristics.

## 4.4 Life Test

The useful life of the recording medium as stored under suitable ambient environmental conditions is a key factor in determining its suitability for mass storage applications. A preliminary investigation into the archival properties of tellurium and bismuth films was initiated under the program. The results are reported in Appendix A. The primary objective of the effort was to establish, within the time interval available to the program, some preliminary indications for the projected lifespan

of the recording materials by means of a series of controlled experiments done at various elevated temperatues. The technique, known as temperature stress aging, is commonly used within the semiconductor industry to obtain some rough indications of device failure rates. Its theoretical validity rests on the assumption of first-order kinetics and the characterization of the degradation process by a single activation energy. For complex phenomena such as laser micromachining, the extrapolated results from accelerated testing should therefore be used with prudence.

Subject to the above caveats, experiments were conducted at four different temperatures, viz., 90°C, 75°C, 55°C and 25°C. The parameters measured were static sensitivity and film reflectance and transmittance. Both tellurium and bismuth films, on PMMA and on glass, were studied. Results on static sensitivity, which give an indication of shelf life, suggest that the degradation process is indeed more complex than what would be expect from single-order kinetics. Humidity, an uncontrolled variable in the experiments, probably plays an important role. The results indicate that the shelf life for tellurium on PMMA is better than 10 years under dry conditions. No significant changes in the optical properties of tellurium films were measured over the time interval for the experiments, projecting an archival life of the recorded film of better than 10 years, assuming simple oxidation to be the dominant degradation mechanism.

## 5.    DISC SUBSTRATE MATERIAL

### 5.1    Investigation

Various materials were considered for the disc substrate.
Selection of the substrate materials, and their dimensions, was
governed by system constraints on the following factors:

- Transverse displacement of film plane.
- Radial displacement of information tracks.
- Adherence of DRAW film to substrate.
- Surface roughness of substrate.
- Energy loss to substrate during recording.
- Birefringence of substrate.
- Thickness of substrate.
- Transparency of substrate.
- Flatness of substrate.
- Relative reflectivity of pit with respect to film.
- Disc speed.
- Handleability of disc.

The most promising material was polymethylmethacrylate (PMMA)
which was supplied in cast sheet form by Glasflex Corporation,
Stirling, N.J.   PMMA is known by various trade names, such as
"Plexiglas", "Perspex", and "Lucite".

Glass, PMMA, and PVC materials were initially selected as
possible candidates for fabricating DRAW discs.   Selection was
based on optical transparency, roughness, flatness, and thickness.

Surface flatness measurements were made with a flatness tester
using a electromagnetic probe.   At random areas, small sections
22 mm square were selected from large samples of commercially
available materials.   For all materials, the flatness varied
from 0.001 $\mu$m to 0.190 $\mu$m (see Table 1).

32

TABLE 1: Surface flatness measurements.

| Material | Manufacturer | Thickness (mm) | Warp (77 cm² Area) (mm) | Surface Flatness (6.5 cm² Area) (µm) | "SEM" Roughness (0.1 cm² Area) |
|----------|--------------|----------------|--------------------------|--------------------------------------|--------------------------------|
| PMMA | Glasflex Corp. | 0.96 | 0.05 to 0.6 | 0.001 | No irregularities appeared |
| Polycarbonate | Westlake Plastics Co. | 0.94 | 0.09 to 0.6 | 0.025 | No irregularities appeared |
| Polysulfone | Westlake Plastics Co. | 0.76 | 0.03 to 0.2 | 0.045 | 0.3 - 0.8 um dia. w/0.2 um depth, scattered |
| Microglass | Corning Glass Works | 0.54 | | 1.00 | |
| CTA 53 | Corning Glass Works | 0.125 | | 0.14 | 0.5 um pits, scattered |
| PVC 25 | Corning Glass Works | 0.200 | | 0.090 | 0.3 - 0.4 µm, scattered bumps |
| PVC | Zenith Corp. | 0.170 | | 0.100 | 0.2 - 0.8 um dia. w/0.1 um high bumps |
| *H-911 (CR-39) | Homalite Corp. | 1.190 | | | |
| Elastotherm (PVC 14) | Phillips Films Co., Inc. | 0.152 | | 0.110 | |
| PVC 11 | Phillips Films Co., Inc. | 0.140 | | 0.190 | |
| PVC 23 | Phillips Films Co., Inc. | 0.150 | | 0.150 | |
| CA 41 | Phillips Films Co., Inc. | 0.130 | | 0.23 | |
| PET 89 | Phillips Films Co., Inc. | 0.125 | | 0.21 | |
| Melenex-S (polyester) | ICI (United States), Inc. | 0.070 | | 0.24 | |

* Costly material.

Samples were also prepared for examination by a scanning electron microscope. 700 Å of aluminum was deposited on one surface, and the samples were then scanned at magnifications between 6700X and 7000X ($\approx 1.4$ $\mu$m/cm$^2$). Several samples showed scattered irregularities, such as pits and bumps varying in size from 0.2 $\mu$m to 0.8 $\mu$m. The samples of polycarbonate and PMMA from Glasflex Corp. appeared to have no significant surface irregularities.

The protective configuration considered most optimum involves recording through the substrate. This places certain requirements on the acceptable birefringence in the substrate material. Our analysis of birefringence under static conditions showed 1 mm thick PMMA, PVC, and polycarbonate as acceptable substrate materials.

## 5.2     Further Results and Observations on PMMA

Warp measurements made on discs using Glasflex Electroglas Sheet indicated that the warp was 0.05 - 0.6 mm. Figure 11 shows photographs taken through an optical microscope at 160X of the surfaces of the Glasflex Electroglas Sheet (homopolymer) and Glasflex Electroglas Sheet No. 2 (co-polymer).

Polymethylmethacrylate was also one of the more birefringent-free and creep-resistant plastics analyzed. Glasflex Electroglas Sheet appeared to be nearly isotropic and attained a creep plateau of about 0.01% in about 100 minutes after the application of a 25 N/cm$^2$ stress. The stress level used corresponded to a typical stress component acting in a disc spinning at 1800 rpm.

Excessive variations in thickness measured on the Glasflex material were of some concern. Such variations made it difficult to compensate the light path. In addition, this caused variations in local stiffness, giving rise to irregularities in the axial deflection of the film plane around the circumference, and also made fabrication more difficult. The problem of thickness

34
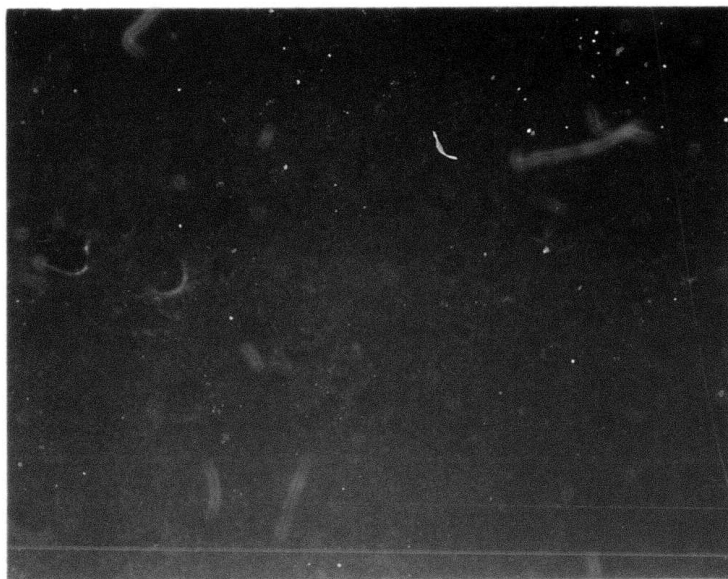
(a) Glasflex Electroglas Sheet (homopolymer).



(b) Glasflex Electroglas Sheet No. 2 (copolymer).

Figure 11:  Surface character of Glasflex
Electroglas Sheets using optical microscope.
(Mag. 160X).

35

variations in excess of the normal manufacturer's specification ($\pm$ 12.5%) was discussed with officials of the Glasflex Corporation. An agreement was reached which resulted in a considerable improvement in quality control (see Appendix B of Ref. 8).

A second source of optical-quality, 1 mm thick PMMA was also found. Rohm and Haas Corporation casts such sheet but generally only in large volumes. In cooperation with NVP, we were able to secure a regular allotment of the material. The samples received were more uniform in thickness than the Glasflex Electroglas Sheet ($\pm$ 4% as opposed to $\pm$ 13%).

## 6.    DISC PROTECTIVE MECHANISMS

### 6.1    General Considerations

Some means of protecting the DRAW film material from scratches, dust, and fingerprints is required before, during, and after writing. According to Bogels (Ref. 1), a 400 $\mu$m protective separation from the information sufficiently defocuses the imperfections to maintain the desired MTF for the home entertainment system (NA = .45).  If h is the distance above the information to sufficiently defocus, then it can be shown by geometrical construction that:

$$h \simeq [200 \sqrt{\frac{1-(NA)^2}{(NA)^2}}]\ \mu m$$

It is interesting to note that to this first approximation the critical height is not a function of wavelength $\lambda$.  For a NA = 0.55 lens, $h_{.55}$ = 305 $\mu$m,  and $h_{.75}$ = 177 $\mu$m.  The most convenient protective mechanism would be to use the disc substrate itself, as is done in the Philips/MCA system.  However, this would require the objective lens to be custom-designed.

The use of a 175 $\mu$m foil as the substrate appeared interesting since it might offer sufficient protection to allow the use of a standard NA = 0.75 microscope objective.  The foil, however, would offer little support to the information layer, possibly causing cracks and other damage.  Also, foils are difficult to handle and have been found to be less flat then the normal 1.1 mm videodisc.

### 6.2    Coatings

Another concept considered was the spinning or dip coating of a thin clear polymer layer on top of the information layer.  Such a polymer layer must adhere to the information layer well enough to produce a good optical interface.  Careful spin, dip or roller

coating would be sufficient; however, it is unlikely that gluing or pressing a thin protective sheet onto the film would be satisfactory.

A 20 μm layer is the minimum thickness that would protect the information layer from scratch damage, but is not thick enough to allow writing through fingerprints and dust. A 175 μm layer would be thick enough for writing with a 0.75 numerical aperture lens, but spinning on such a thick layer would be difficult. It may be possible to dip coat a 175 μm uniform layer.

Workers at NVP and at PL found that writing through thin polymer layers is possible, but bubbles form which make top-side readback unlikely. Figure 12 is an edge view of the situation after writing, showing the information-layer material supported by the disc substrate and covered by a thin layer of Perspex or Cellosize. The heat of writing vaporized and melted the information layer to form a pit, damaged the plastic substrate material, and caused a bubble to form above the pit. Readback of the pit edges through the topside is unlikely due to inter-ference and aberration effects of the bubble. It is possible
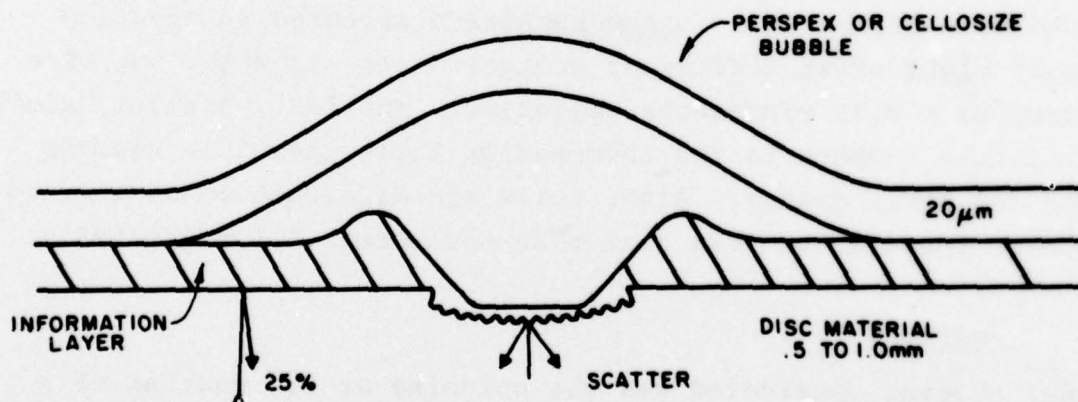


Figure 12: Profile of disc showing bubbles formed by writing through a protective layer (not to scale).

that backside readout can be accomplished as long as substrate damage is small. An evaluation was carried out to investigate the decrease in material sensitivity with the application of an overcoating (see Appendix C of Ref. 9). A loss in sensitivity was observed.

A second possible protective mechanism would be to write top-side on a bare information layer and then spin, dip, spray, or glue on some simple protective coating. The discs could be protected before writing by a similar layer which could be removed or peeled off just before writing. One advantage of this method over the permanent polymer layer is that no bubbles would be formed. However, this would not be important unless one desired to read back from the topside of the disc. A 400 $\mu$m clear layer would be acceptable assuming it could be properly applied to achieve a good optical contact with the information layer. Three drawbacks of this method are that any vapor generated during the writing process may: coat the objective, contaminate the atmosphere, and require additional handling after writing to assure dust and fingerprint protection.

## 6.3    Air Flap

The use of an air-bearing foil or "flap" as a protective layer for the optical disc was proposed. Figure 13 is a profile of a disc coated with an information layer protected by a thin optically homogeneous foil having relatively large flatness and thickness tolerances. The foil cover is attached only at the center of the substrate where some means of providing a radial air flow from the inner to the outer radius is accomplished by either spokes or a circle of concentric holes. As the flap and sub-strate rotate, a uniform radial air bearing is formed lifting the flap off the information surface. It is expected that the flap would have many advantages over other techniques for dust, fingerprint, and scratch protection, such as:
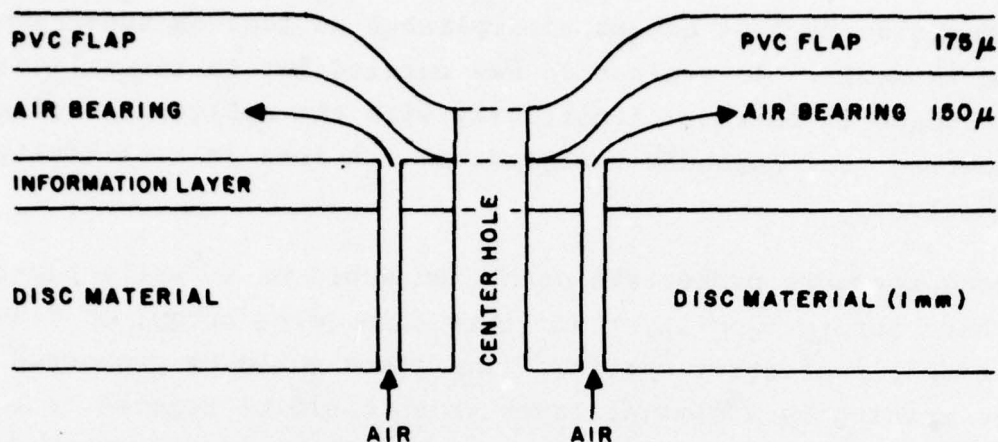
Figure 13: Air bearing foil (flap) protection (not to scale).

- The disc substrate may be chosen for its flatness and strength without regard for its optical properties.

- During writing, any vaporization products will deposit on the foil and be prevented from coating the objective lens. It is expected that any deposition will be less than 100 A and completely transparent during reading.

- Electrostatic charges will hold the flap in contact with the disc when the disc is not rotating, thereby providing scratch protection.

- The protective foil could be renewed if necessary.

Readback in reflection through such a disc/foil configuration produced results identical to normal videodisc operation. It is possible that a 175 $\mu$m foil could be written and read through by topside reflection with a standard microscope objective normally compensated for cover glass. By employing a 150 $\mu$m air bearing support and rather flat foil, it may be possible to use an objective with a working distance of 500 $\mu$m or less.

40

## 6.4    Laminates

Various combinations of laminated materials were considered in relation to strength, creep resistance, compactness, and integrity of the stored information.  The disc substrate may be optimized for its strength, creep resistance, and thermal diffusivity.  The recording material may be deposited on the substrate or on the protective cover, whichever is more suitable. The protective cover may be glass or clear plastic, for example, if writing or reading is to be performed through it.  Of course, the disc substrate must also be transparent if writing or reading is to be performed through it.  The increase in recording power required for some laminate structures was evaluated (see Appendix C of Ref. 9).  A loss in sensitivity of as much as a factor of 2 was observed, making such laminates undesirable as protective mechanisms.

Straining of the substrate and the protective layer due to mechanical and thermal stresses must be closely matched to prevent warping.  This matching may be achieved by material selection.

Scratch protection can be obtained with a very thin (20 $\mu$m) protective cover, while defocusing of dust, etc. would require a thicker (400 $\mu$m) cover.

Precise centering of the disc can be accomplished by having a concentric boss in the center of the record.  This, however, may create stacking problems.  Another option would be to have the disc flat, smooth, and with no holes, and to center it by using a lip or ridge on the outer diameter of the turntable.  This design would cause the disc to be self-centering in a reproducible way and would also reduce creep.

To summarize, the primary objections to the use of a laminate are loss of recording sensitivity and difficulty of manufacture.

## 6.5   Air Sandwich

The "air sandwich" protective mechanism shown in Figure 14 consists of two discs, each coated with an information-sensitive layer, separated by spacers (ring gaskets) at the inner and outer radii of the information band.   Two configurations are possible.   The potential advantages of the air sandwich design are:   protection of the information layers without degrading writing sensitivity, containment of any writing byproducts, and a *double sided disc*.   It *should be noted* that solid-film contact should be minimized for maximum writing sensitivity and playback fidelity.   In the air sandwich design, there is solid-film contact with only one side of the recording film.

Since the air sandwich appeared to be the most attractive mechanism for protecting the disc, it was selected as the prime candidate for extensive analysis and testing.   A detailed analysis of the air sandwich is presented in Appendixes I and II of Ref. 10.   The analysis predicts a well behaved structure that would meet the program requirements.
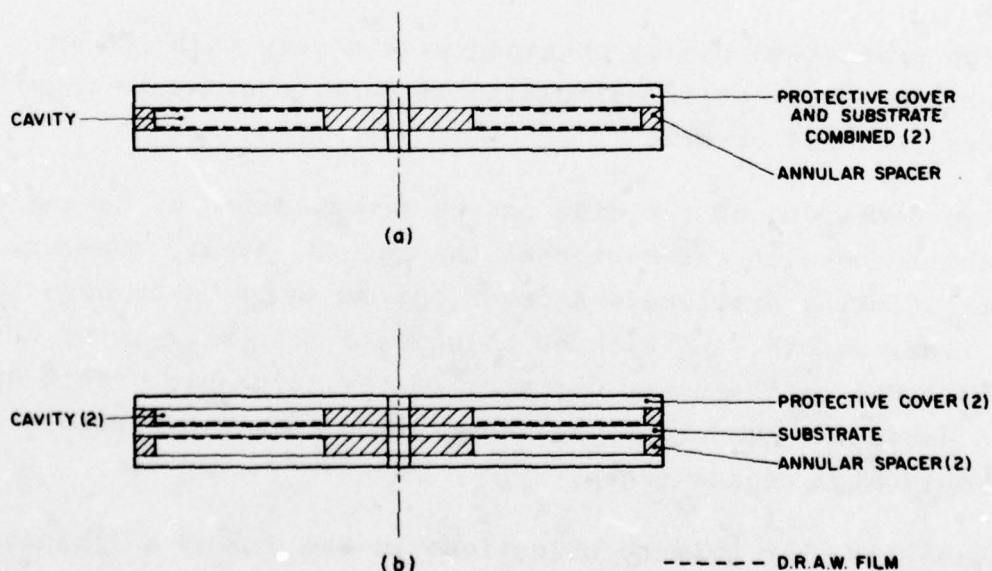
CAVITY — PROTECTIVE COVER AND SUBSTRATE COMBINED (2) — ANNULAR SPACER

(a)

CAVITY (2) — PROTECTIVE COVER (2) — SUBSTRATE — ANNULAR SPACER (2)

(b)          - - - - - D.R.A.W. FILM

Figure 14:   Alternate air sandwich configurations.

# 7. AIR SANDWICH DESIGN AND FABRICATION

## 7.1 Dimensions

Since the disc may be spun at 30 rps, it seemed worthwhile to consider a disc design capable of both 3 rps and 30 rps operation. Four areas were considered in optimizing the disc dimensions, viz., cavity thickness, spindle-hole diameter, turntable support surface, and static balancing. It did not appear that the dimensions and fabrication of a dual-speed disc would be significantly different from a disc intended strictly for 3-4 rps operation. The primary differences are in the cavity thickness and balance requirements. The cavity thickness required to prevent the film planes from touching while spinning depends on such things as the inside diameter of the cavity, the turntable support dimensions, and the speed of operation. The inside diameter of the cavity and the turntable support dimensions are, in turn, set by other subsystem considerations such as the dimensions of the sled and focus motor. With the hardware developed, the inner cavity diameter and the outer diameter of the disc adapter on the turntable can be set as large as 6.5 cm and 3.8 cm, respectively. Under these conditions, the disc is so stiff that the theoretical cavity thickness required to prevent the film planes from touching in a disc of the configuration shown in Fig. 14a, is less than the typical unflatness (0.1-0.2 mm) of the film plane. This is true even for 30 rps operation. The net result is that the cavity thickness can be selected so that there will be no contact of the films during "normal" handling of the disc. The cavity thickness required for such a purpose is 0.25-0.5 mm. The static balance requirement is much more severe for high-speed operation than for low-speed. The balance specification was tentatively set to be the same as that for a videodisc ($\leq$ 4 1/4 gm-cm).

The spindle hole diameter was also standardized at 35 mm, the same as that of a consumer videodisc. The inner and outer radii of the air cavity are 6.5 cm and 14.5 cm, respectively. The

inner radius was chosen as large as possible, and the outer
radius as small as possible, to provide maximum flexural stiffness.
The diameter of the disc adaptor on the turntable can be as large
as 9 cm (with the present focus motor) to provide maximum support
for the disc.  Calculations have shown that under these conditions
the average outer edge static droop of an air sandwich would be
0.17 mm.

## 7.2    Fabrication

A disc assembler was designed and built during the program (see
Fig. 15).  It is capable of mechanically implementing all of the
adhesive assembly techniques that we had developed.  Basically,
it consists of two vacuum hold-down plates which can be guided
together in a parallel fashion by means of a four-bar linkage.
Once in contact, the plates can be pneumatically subjected to a
predetermined load.  The maximum clamping force attainable is
about 6600 N.  The plates serve to hold the substrates and
standoffs flat as the disc is laminated together.  The lower
vacuum plate and an auxiliary plate also serve to align the
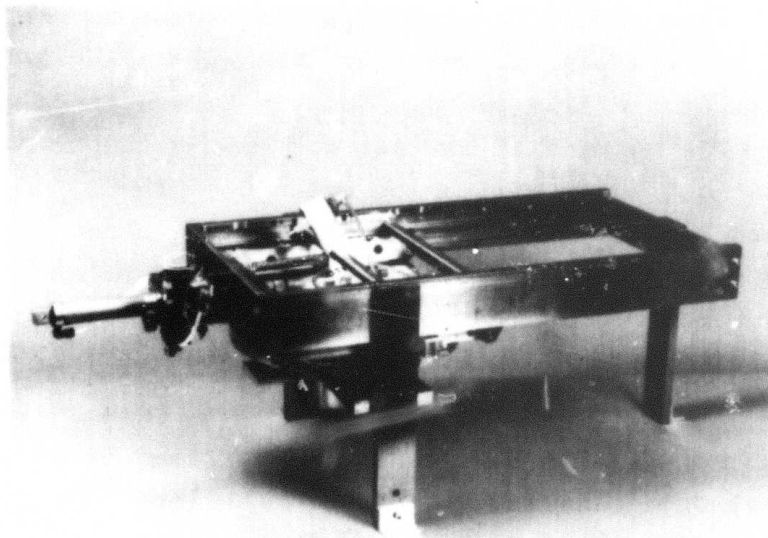substrates and spacers concentrically.  The adhesive is dispensed



Figure 15:  Assembler for air-sandwich DRAW discs.

from a pneumatically controlled hypodermic syringe. An upper guide serves to bring the dispenser into position as well as hold it in a standby location off to the side of the vacuum plates. The syringe is indexed into position over the outer and inner spacer zones. As the lower vacuum plate is rotated by means of an electric motor the adhesive is automatically dispensed during one complete revolution.

A technique was developed for solvent cementing the disc components. Obtaining a uniform bond throughout both joints of an air sandwich is particularly difficult with solvents since they tend to wick onto undesired surfaces of the disc and assembly fixtures. However, the joints that result from the use of certain solvents are extremely strong and clear. The technique developed is illustrated in Figure 16.

The inner and outer spacers are held flat and concentric by means of a guide plate (Fig. 16a). A puddle of solvent is placed on the inner spacer, and a tellurium-coated substrate is lowered into contact with the puddle. The substrate is held with a vacuum plate and bulged out slightly by means of a spring-loaded plunger protruding through the center of the plate. As the bulge contacts the puddle, a meniscus is formed which is concentric with the axis of the disc. Further clamping of the guide and vacuum plates flattens the bulge, thereby spreading the solvent to the outer edge of the spacer. Solvent is then wicked in between the outer spacer and substrate by moving a hypodermic needle around the outer edge of the disc (Fig. 16b). The outer diameter of the outer spacer is 1 to 3 mm larger than that of the substrate. The step formed by the difference in diameters provides a guide for the needle and prevents solvent from wicking between the guide plate and the spacer. The resulting assembly is then turned over and held down to the lower vacuum plate. The second substrate is cemented into place by repeating the above procedure (Fig. 16c).

The best solvent tested was the unpolymerized methyl-methacrylate monomer from which the Glasflex Electroglas

45

SPRING LOADED
PUSH BAR

UPPER VACUUM
PLATE

TELLURIUM
COATED
SUBSTRATE

SOLVENT
PUDDLE

OUTER SPACER

SPACER GUIDE
PLATE

INNER SPACER

(a)

HYPODERMIC
NEEDLE

(b)

TELLURIUM
COATED
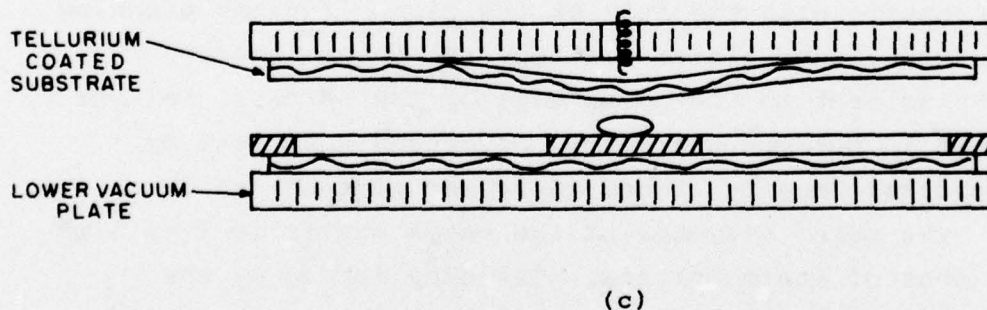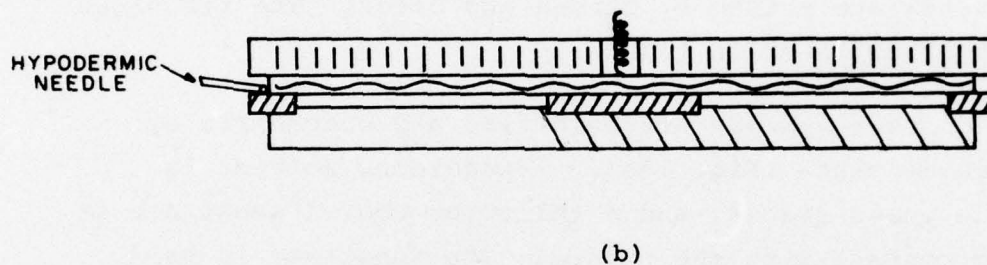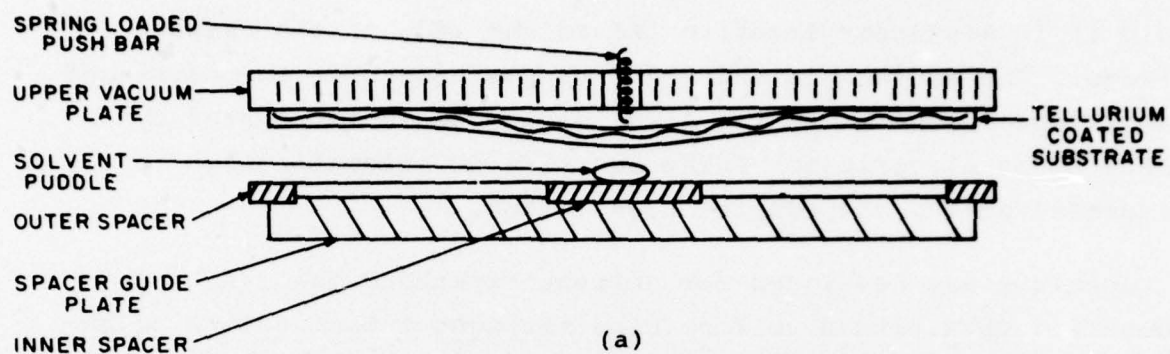SUBSTRATE

LOWER VACUUM
PLATE

(c)

Figure 16: Solvent cementing technique for air-sandwich discs.

substrate was made.  The resulting joint was very clear and at
least as strong as the substrates.

## 7.3     Alternate Disc Hubs

Two new types of disc hubs were studied.  One basic idea was to
replace the entire label area of the disc with a steel plate
containing the 35 mm spindle hole (Fig. 17).  The plate
would also serve as the inner spacer.  Such a design has many
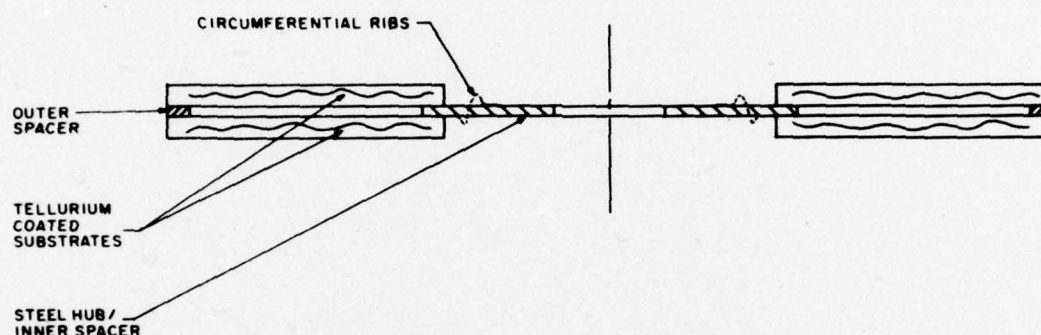advantages.



Figure 17:   Alternate hub configuration
(metal hub, 35 mm diam. hole).

Disc assembly is particularly simple.  A low viscosity cyano-
acrylate adhesive such as Permabond 101 readily wicks into the
gaps between the plate and the substrates.  The plate, with its
prefinished spindle hole, can be bonded in place so as to locate
the center of the spindle hole on the mass center of the final
assembly.

All of the plate dimensions (spindle hole, spindle hole position,
thickness, flatness, and outer diameter) can be controlled much
more precisely with metal rather than plastic.  Therefore,
within the tolerance of the plate-thickness variations (typically
less than $\pm$ 25 $\mu$m), the location of the disc parallel to the
axis of the turntable is referenced to the nominal film plane
and thereby becomes nearly independent of variations in substrate
thickness (typically $\pm$ 125 $\mu$m).  And, insofar as the flatness

47

of the disc is determined by the flatness and stiffness of the hub, it should be possible to make the disc flatter.  For example, the flatness and stiffness of a metal plate can be significantly increased by stamping circumferential ribs into it (Fig. 17).  One would also expect that the disc with the metal hub would be more dimensionally stable, when subjected to temperature and humidity variations, than one with a plastic hub.  Finally, a steel hub would permit the disc to be clamped magnetically, if desired.

## 8.    ELECTRONIC SIGNAL PROCESSING SYSTEM

During writing, the electronic signal processing system for the
DRAW recorder encodes the incoming data to provide for error
detection and correction, and then modulates this encoded data
into the format desired for recording on the disc.  During
reading, the system first demodulates and then decodes the data
from the disc.

An experimental signal processing setup was designed, assembled,
and tested to measure the raw error rate and to demonstrate the
capability of continuous data recording and retrieval with a low
error rate.  The system first encodes the data with 256 bits of
interleaving depth and with a triple-error correcting convolu-
tional code, followed by modified frequency modulation (also
known as MFM and Miller) before recording on the disc.  The
Miller code (Ref. 11) was chosen for its high density, required
bandwidth, and low dc content.  Convolutional encoding-decoding
(Ref. 12) was chosen for error correction rather than block
encoding-decoding because it is less complex for the correction
requirement of the optical disc system.  For instance, interleav-
ing can be done easily by using shift registers for convolutional
codes; whereas for block codes, double buffering using two RAMs is
necessary.  Also, decoding for convolutional codes (Ref. 12) is
more straightforward than block codes.  The playback signal is
amplified and processed and demodulated using a phase-lock loop
circuit.  The demodulated data is then decoded by the convolu-
tional decoder.

The block diagram of the experimental setup is shown in Figure 18.
A stable 1 MHz clock is supplied by a frequency synthesizer.
A pseudo-random bit sequence (PRBS) of $2^9-1$ bits with a non-
return-to-zero (NRZ) format was chosen as the data source supplied
(HP3780A pattern generator).  The data is encoded with a
Linkabit LF1011-256 convolutional encoder capable of
correcting triple errors over 22 bits of encoded data.  The
encoded data is then modulated by the Miller modulator and
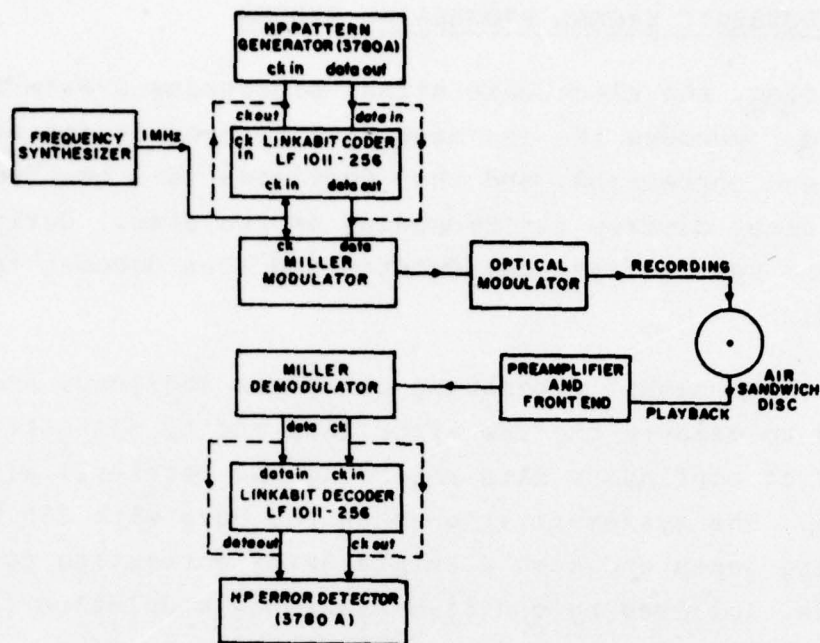recorded on the optical disc.

Figure 18: Setup for measuring data error. (For raw error rate measurement, Linkabit coder/decoder is replaced by dashed connections).

During playback, the reflected light from the read beam is collected by a photodiode which converts it into current. The signal is fed to a preamplifier and front end module which provides amplification, amplitude equalization, and signal detection. In the Miller demodulator, a phaselock loop is used to lock on to the detected data to generate a continuous clock which, together with a phasing circuit, demodulates the signal back to NRZ format. The data are then decoded and de-interleaved by the Linkabit decoder. The regenerated clock and the decoded data are then connected to an error detector (HP3780A) which reinitializes the same pseudo-random bit sequence. The sequence is then compared bit by bit to the decoded data and any differences recorded as errors. Typical waveforms of playback modulated data and the demodulated and decoded NRZ data are shown in Figure 19.

50
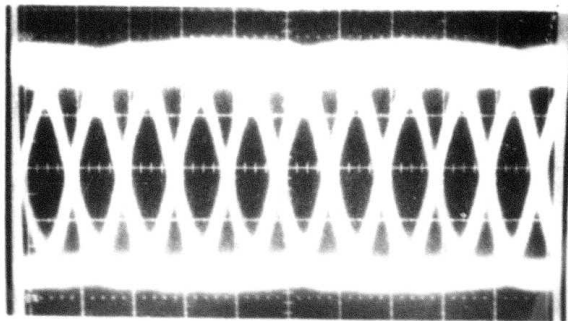
Eye pattern of data off disc.
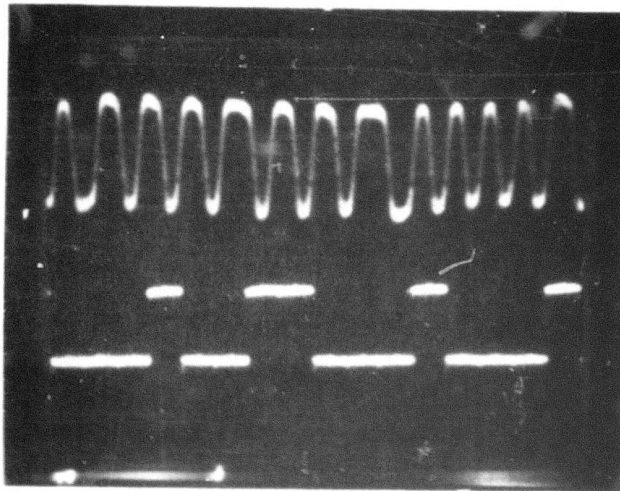
Data off disc.

Demodulated and decoded NRZ data.

Figure 19:   Encoded and corrected data from an air sandwich disc (0.5 Mbit/s data rate).

From the experimental setup, a block of $0.9 \times 10^8$ bits of data was recorded in 3 min, with a data rate of 0.5 Mbit/s.  At playback, the data was measured and found to be error free for 130 sec, i.e., a $0.65 \times 10^8$ bit block of data was successfully retrieved.

Theoretically, with triple-error, convolutional, encoding-decoding, an interleaving depth of 256, and an average pit length of 1.5 $\mu$m per bit, a defect as large as $(3 \times 256 \times 1.5) = 1,152$ $\mu$m, or 1.1 mm, can be tolerated on the disc surface as long as it is not closer than $(22 \times 256 \times 1.5) = 8448$ $\mu$m or 8.4 mm from one another on the same track.  According to Linkabit Corporation (Ref. 1 ), the convolutional encoder/decoder would be capable of achieving error rates of less than $10^{-9}$.

## 9.    RECORDER CONTROL SYSTEMS

### 9.1    Focus Control System

The requirements for storage of high-density information by the DRAW optical system dictate that the optical elements used for producing the read and write spots have a large aperture with a small depth of focus (typically a few microns).  Since the high density of the information is two-dimensional, defocusing of the optical spot at the disc produces a reduction of bandwidth in the tangential (along the track) direction and crosstalk in the radial (perpendicular to track) direction.

Figure 20 shows the effect of defocusing on bandwidth at an inner and outer track (Ref. 1).  Because the information bit length decreases proportionately with track radius for applications of constant angular velocity, the effect is more pronounced at the inner radius.  Figure 21 shows the dependence of crosstalk on track pitch and defocusing (Ref. 1).  Crosstalk of
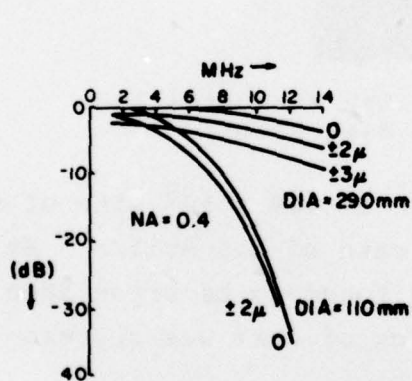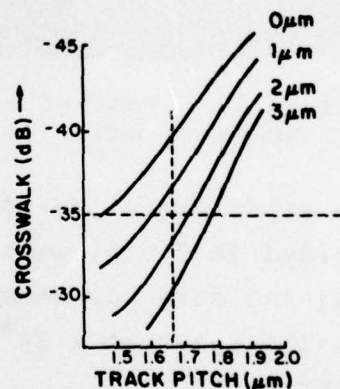
Figure 20:  Effects of defocusing on bandwidth.

Figure 21:  Measured crosstalk vs. track pitch for various amounts of defocusing (NA = 0.40).

- 35 dB is usually acceptable when adjacent tracks have essentially similar information, as in standard television applications. However, in applications where each track contains unique information, crosstalk requirements reduce the allowable focus error

or force a sacrifice of information density by increasing track pitch. These two figures represent performance of a 0.4 numerical aperture system. If small spot sizes are required, the larger numerical aperture will result in reduced defocusing tolerances. For these reasons, a conservative track pitch of 2 $\mu$m was selected.

The amount of defocusing encountered under dynamic conditions with no servo control depends primarily on the type and condition of the substrate material. Factors such as turntable shaft wobble and other mechanical vibrations have a secondary effect.

While glass substrates can be fabricated and maintained to a high degree of flatness, plastic substrates may, as a result of warp and thickness variations, deviate from the ideal disc plane by as much as 500 $\mu$m (Ref. 1). This variation is encountered although centrifugal forces produce some flattening of the disc.

Most of the variation in disc position occurs at the fundamental frequency of rotation; higher frequency variations decrease in amplitude at a rate of 30 to 40 dB per decade. For a rotational speed of 3 rps, a 60 dB open-loop servo gain at 3 Hz is required to compress the expected $\pm$ 500 $\mu$m disc plane variation to a focus error of $\pm$ 0.5 $\mu$m, and the required acceleration of the objective motor is 0.04 g. The resulting closed loop bandwidth is about 300 Hz. For a rotational speed of 30 rps, the acceleration required is increased by a factor of 100 and the bandwidth by a factor of 10. The system was designed to function at both disc speeds.

Figure 22 shows a block diagram of a typical focus servo and its open-loop frequency response. The correction and power amplifiers are standard items, and the linear objective motor is a magnetic-loudspeaker-type movement supported by springs or by an air bearing. The electro-optic focus error detector is described in the following section.
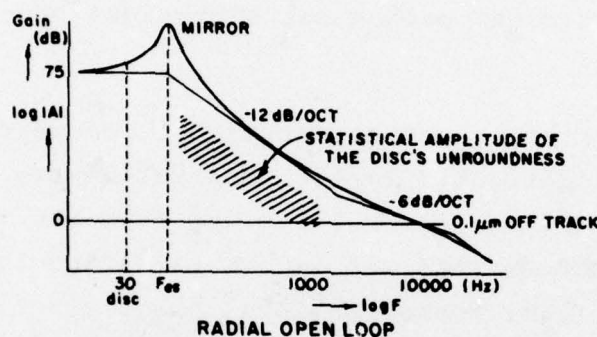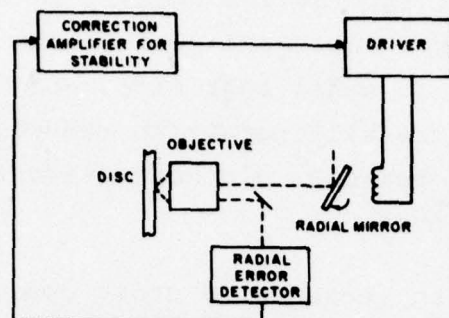
Figure 22: Block diagram of focus control
system and its open-loop frequency response.

### 9.1.1    Focus Error Detection

The focusing method employed in the recorder is known as side-
spot or skew-beam focus.  Referring to Figure 23, an auxiliary
laser beam is imaged through a slit of about 250 $\mu$m so that it
enters the reading objective off-center and off-axis.  This beam
fills only a small portion of the entrance pupil.  As a result,
the spot on the disc is large (20 $\mu$m).  When the system is in
focus, the beam follows path A and exits through the slit.
If the disc is displaced to the right, the beam follows path B
and illuminates photodiode 1.  When the disc is too close, path
C is followed and photodiode 2 is illuminated.  For all disc-to-
objective distances over the operating range, the focus error
signal, which is the difference of the two photodiode currents,
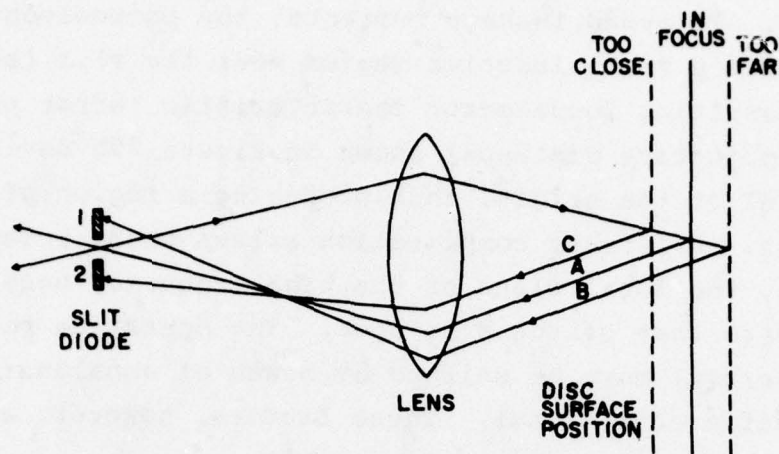will provide both amplitude and direction information.

Figure 23:   Schematic of side-spot focus.

The focus spot is located far from the center of the field-of-view of the objective.  Figure 25 shows the location of the focus spot in the field-of-view, about 40 $\mu$m from center perpendicular to the axis of the radial tracking mirror.  The spot *should be located along the axis of* the radial tracking mirror to prevent modulation of the focus error signal during the large allowable excursions of the radial tracking mirror.
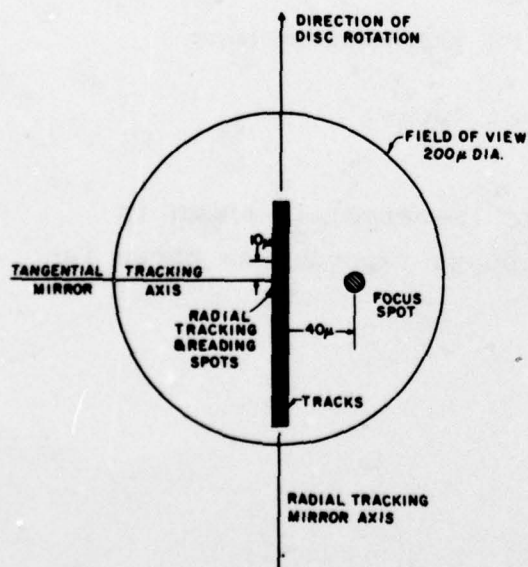


Figure 24:   Location of focus spot in field-of-view.

There are two other factors which may degrade the side-spot focus system. To avoid leakage currents, the photodiodes are fabricated with a small inactive region near the slit (see Fig. 25a). The resulting focus-error characteristic (error current vs. disc-to-objective distance) shown in Figure 25b deviates from the ideal at the origin, thus producing a region of low gain at focus. A further complication arises when, because of misalignment, the focal plane of the high frequency beam is not coincident with that of the side spot. The operating point (zero focus error) must be shifted by means of unbalancing the photodiode difference signal. These factors, however, are eliminated by careful design and assembly.



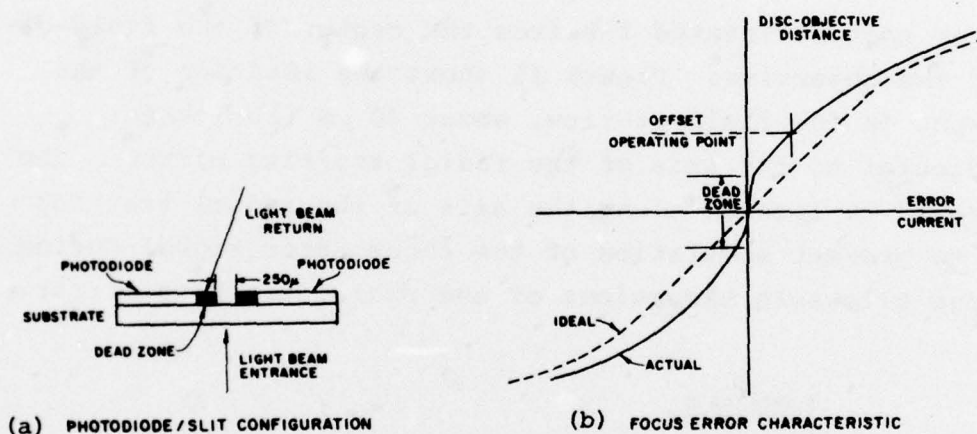(a) PHOTODIODE/SLIT CONFIGURATION          (b) FOCUS ERROR CHARACTERISTIC

Figure 25: Side spot focus.

A typical focus error characteristic (S-curve) is shown in Figure 26 the S-curve for the prototype recorder is shown in Figure 27.
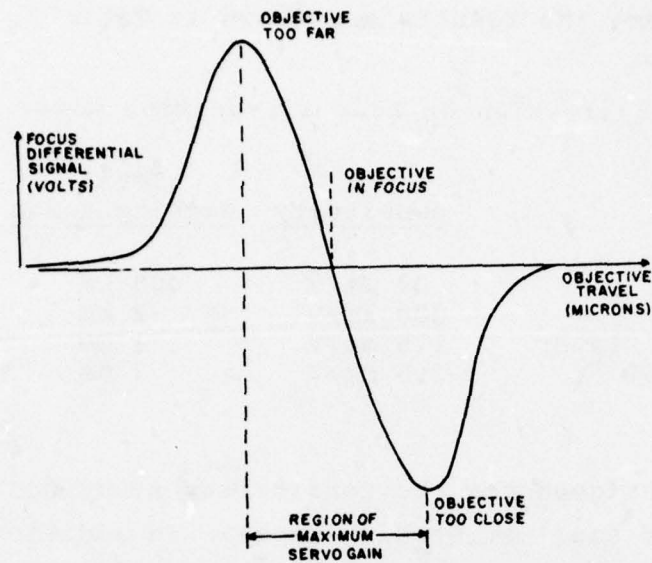
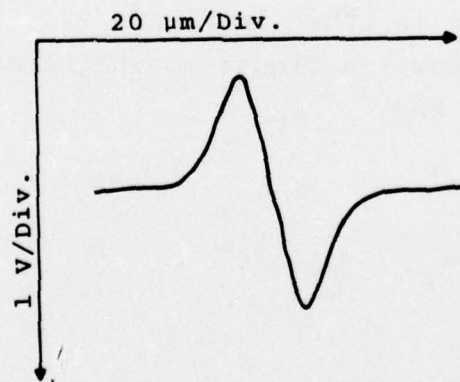Figure 26:  Typical focus error characteristics.



Figure 27:  Focus error characteristic of prototype recorder.

### 9.1.2  Focus Servo

Four designs for an air-bearing focus motor were evaluated
for the recorder; the results are shown in Table 2.

TABLE 2:  Evaluation of four air-bearing motor designs.

| Motor Type | Sensitvity | Total Working Range | Bearing Stiffness |
|---|---|---|---|
| PL | 30 $\mu$m/V | 400 $\mu$m | good |
| NVP | 300 $\mu$m/V | 2 mm | good |
| Integrator Player | 1.5 mm/V | 1 mm | poor |
| Modified NVP | 2.5 mm/V | 2 mm | good |

The PL motor designed for the feasibility study had the lowest
sensitivity and smallest working range.  In addition, spring
suspension caused a mechanical resonance to occur at about 2
kHz.  The modified NVP motor was selected for use in the recorder.
The increased sensitivity of this motor over the standard NVP
resulted from the use of samarium-cobalt magnets and reduction
of the weight of the moving carrier and coil resistance.

The frequency response of the motor is shown in Figure 28.
Above 20 Hz, the response decreases at a rate of 40 dB/decade so
that simple lead compensation is sufficient for the servo.  The
basic servo amplifier is shown in Figure 29.  The system closed-
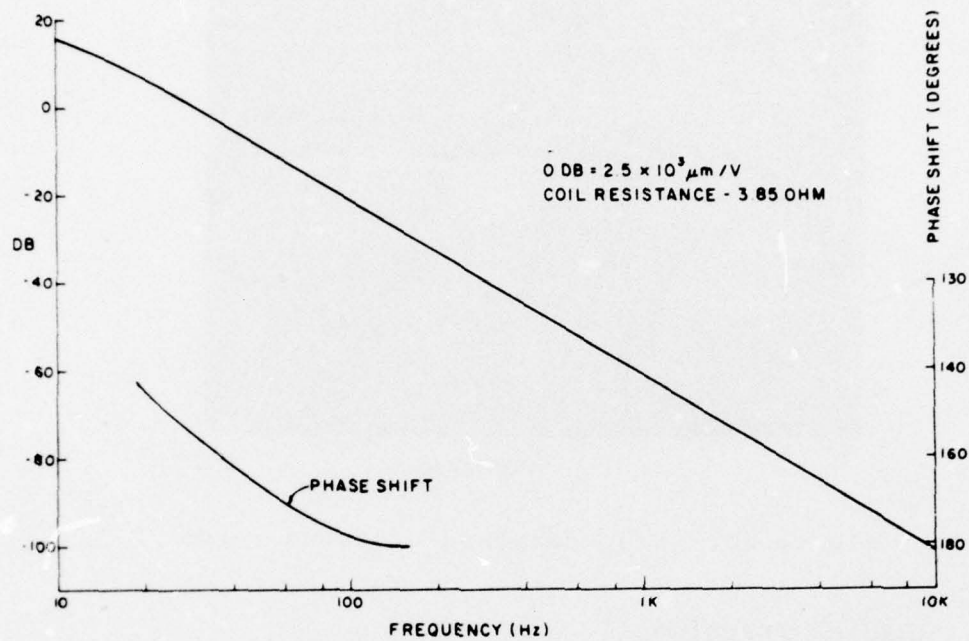loop step response shown in Figure 30 indicates that the
bandwidth is about 2 kHz.

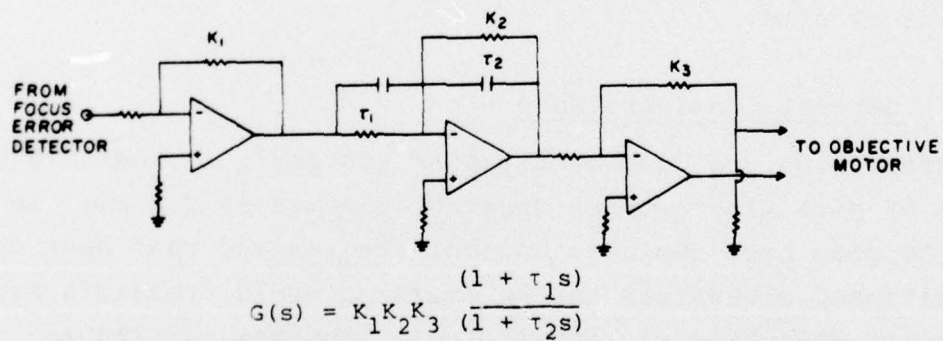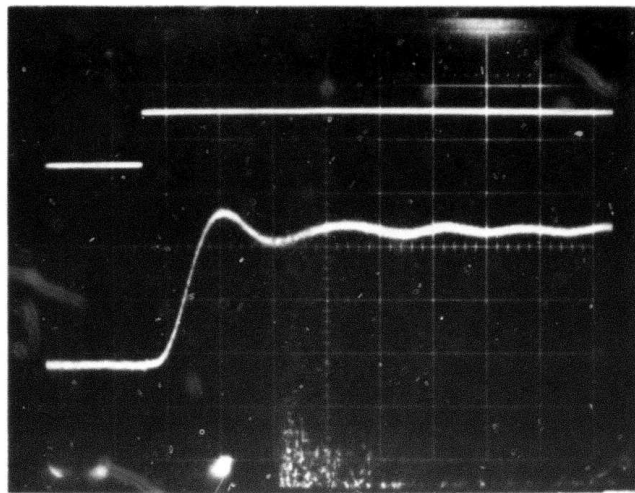Figure 28: Frequency response of modified NVP objective motor.



$$G(s) = K_1 K_2 K_3 \frac{(1 + \tau_1 s)}{(1 + \tau_2 s)}$$

Figure 29: Focus servo amplifier.

500 μs/div.

Figure 30:   Step response of focus servo.

## 9.2     Radial Tracking

This section describes the general considerations and specific
error detecting techniques for radial tracking of the read beam
during playback of the DRAW recording.  The requirements for
radial tracking and focusing are determined by the same factors,
viz., disc flatness and mechanical deviations in the turntable
and optical sled.

### 9.2.1    General Considerations

The information recorded by the DRAW system is in the form of a
spiral of pits with a track spacing or pitch of 2.0 $\mu$m.   In
order to play back the information, the focused read beam must
be positioned accurately on the track to avoid crosstalk between
tracks and reduction of signal level.   The maximum radial
(tracking) error allowed for crosstalk level of - 35 dB accept-
able for television type signal is 0.3 $\mu$m when the track
spacing is 2.0 $\mu$m.   This allowable error is reduced when the
information on each track is unique.   For larger track spacing,
the effect of crosstalk is diminished but the loss of infor-

60

mation signal level as a function of radial error remains. For a 0.3 μm radial error, the information signal level is reduced by about 3 dB.

Because the read and write beams share the same optical system, the expected uncompensated radial error in the DRAW mode of operation is small and may be within the above-mentioned limit. In the playback mode, the uncompensated error of a system using plastic discs is substantial and can be attributed to warping of the material initially and during storage and to flutter resulting from mechanical and aerodynamic effects.

The worst-case uncompensated error, referred to loosely as track eccentricity, is about 30 μm at the fundamental rotational frequency of 3 Hz with higher frequency components decreasing at a rate 40 dB per decade.

The correction mechanism used to reduce the radial error to within allowable limits is a pivoting mirror in the back focal region of the objective which supplies small angular displacements of the read beam of about 0.01° per μm of eccentricity. The mirror is suspended in the moving coil of a galvanometer of low resonant frequency (typically 100 Hz).

Figure 31 shows the block diagram of a typical radial error servo and the open loop frequency response of the system at maximum disc rotational speed. The roll-off of the mirror characteristic and that of the expected radial error frequency components are essentially identical. The next section describes the technique for radial-error detection.

### 9.2.2   Radial Error Detection

A brief description of the radial tracking error-detecting method, known as two-spot tracking, is presented here. This tracking method, used on the NVP and PL recorders, relies on comparing the reflectivity of the disc on both sides of the
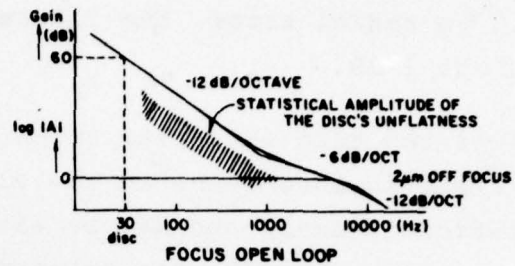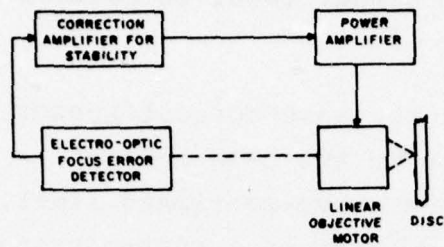
Figure 31:  Block diagram of radial tracking
servo and open-loop frequency response.

track being read.  A light beam is focused on each side of the
track, and the tracking error signal is the difference of two
photocell currents derived from the reflection of each beam.
Since the average reflectivity of the track is less than the
reflectivity between tracks, a non-zero difference signal is
produced if the distances between the center of the track and
the center of the tracking spots are unequal.  The form which
the signal takes is illustrated in Figure 32 for one-half
revolution of the disc without servo control.  Because of the
eccentricity, a number of tracks pass continuously over the two
spots of light.  In this case, 32 tracks pass the spots, so that
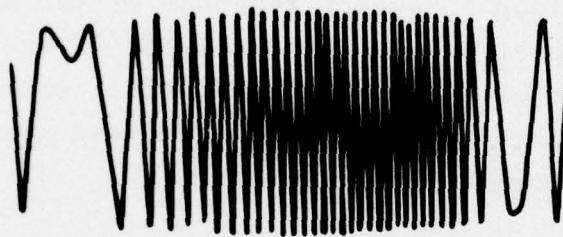the eccentricity is apparently 64 $\mu$m (2 $\mu$m track pitch).

Figure 32:  Open loop (uncompensated)
radial error signal.

As shown in Figure 33, the two tracking spots on the disc are
separated from the signal detecting spot in the tangential
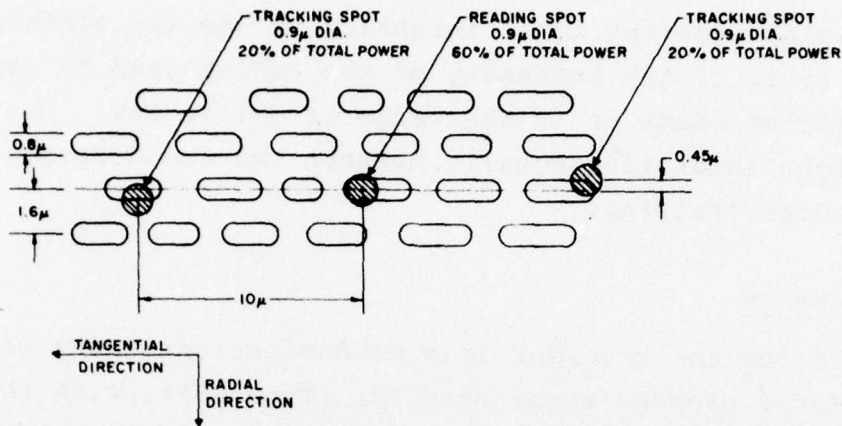


Figure 33: Location on disc of reading
and radial tracking spots.

direction by about 10 $\mu$m to avoid crosstalk between video and
tracking channels.  In the radial direction, the tracking spots
are displaced by about 0.5 $\mu$m from the center of the reading
spot, so that under the conditions of radial tracking (as shown)
the average reflected light from each spot is between the
minimum expected from the track and the maximum expected from
the region between tracks.  This ensures high servo gain near
zero radial error.

The optical schematic of Figure 34 shows that the incoming laser
beam is converted into a three-beam array by a square-wave phase
grating of about 24 $\mu$m line width and 0.2 $\mu$m line depth.
Generation of the three beams by a grating ensures a fixed and



Figure 34:  Optical schematic of two-spot
radial tracking.

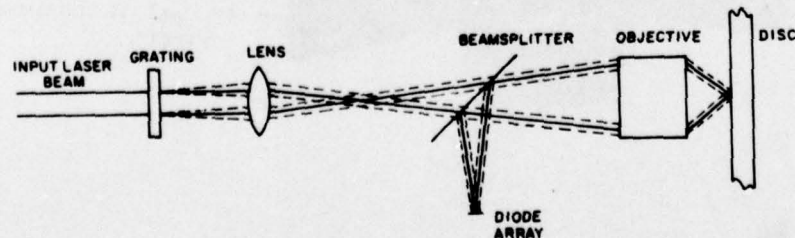predictable separation of the beam in the tangential direction. The radial displacement is achieved by rotation of the grating about the optical axis.

The grating also provides equal intensity of the two tracking beams. The ratio of the intensity of the center beam to each of the diffracted beams is in the range of 3:1 to 1:1. The remaining light is divided equally between the two diffracted beams for radial tracking.

## 9.3    Turntable

The turntable for the recorder is a dc device consisting of a Kollmorgen Corp. pancake armature motor (Type U9M4) with the ball bearings removed and replaced by a Professional Instruments rotary air bearing (Model 4B). The air bearing is directly coupled to one end of the motor shaft. A 2000 line optical encoder dial and single pickoff are mounted on the other end of the motor. The turntable is shown in Figure 35. At 3 rps, the radial wobble of the spindle at the disc adaptor is less than the resolution of the equipment ($< 0.05 \ \mu$m).
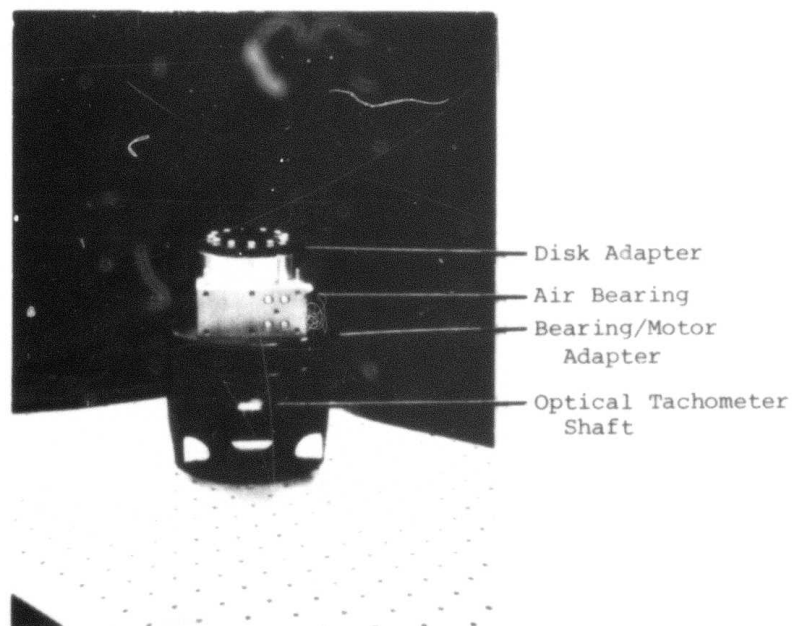


Figure 35:    DRAW recorder turntable.

64

Speed control of better than 0.1% short term and 0.01% long term is attained by building a phase-locked loop around the motor using a crystal-derived reference frequency. Phase lock is established by phase comparison of the reference frequency and the frequency generated by the optical shaft angle encoder. A detailed description of this servo is given in Appendix B.

## 9.4    Sled Servo

The sled is an essentially frictionless device for translating the recording optics to produce a spiral information track on the disc. As shown in Figure 36, the sled consists of a Dover special air bearing of rectangular cross section (Model 400B) with jeweled orfices, a linear dc electric motor, and a linear velocity transducer (Collins LMV-719-S22).

The linear motor is capable of producing a force of about 2 N and is able to remove the bearing collar over a travel of 10 cm in less than 0.5 s.

The velocity of the sled during recording is held constant to within 10% by a servo. The instantaneous velocity is sensed by the inductive velocity transducer, which produces a proportional voltage for servoing the motor to a constant velocity. The system, tested at the component level, operates reliably at constant velocities as low as 1 $\mu$m/s.

Uniform sled-motor speed at 6 $\mu$m/sec is critical to the concept of an inexpensive recorder using a low powered laser. These first tests indicated that sled-motion uniformity satisfies the design goals.

The laser power directly determines the recorder bit rate, disc speed, and arm speed of the sled. As more power is available for recording, shorter exposure times are needed to machine a hole. A shorter exposure time enables recording at a higher

data rate. To maintain the minimum pit size of 1 $\mu$m, an increased data rate requires a proportional increase in disc speed. To maintain a track spacing of 2 $\mu$m, an increased disc speed requires an equal increase in sled speed. A complete analysis and report on performance are given in Appendix A of Reference 14.
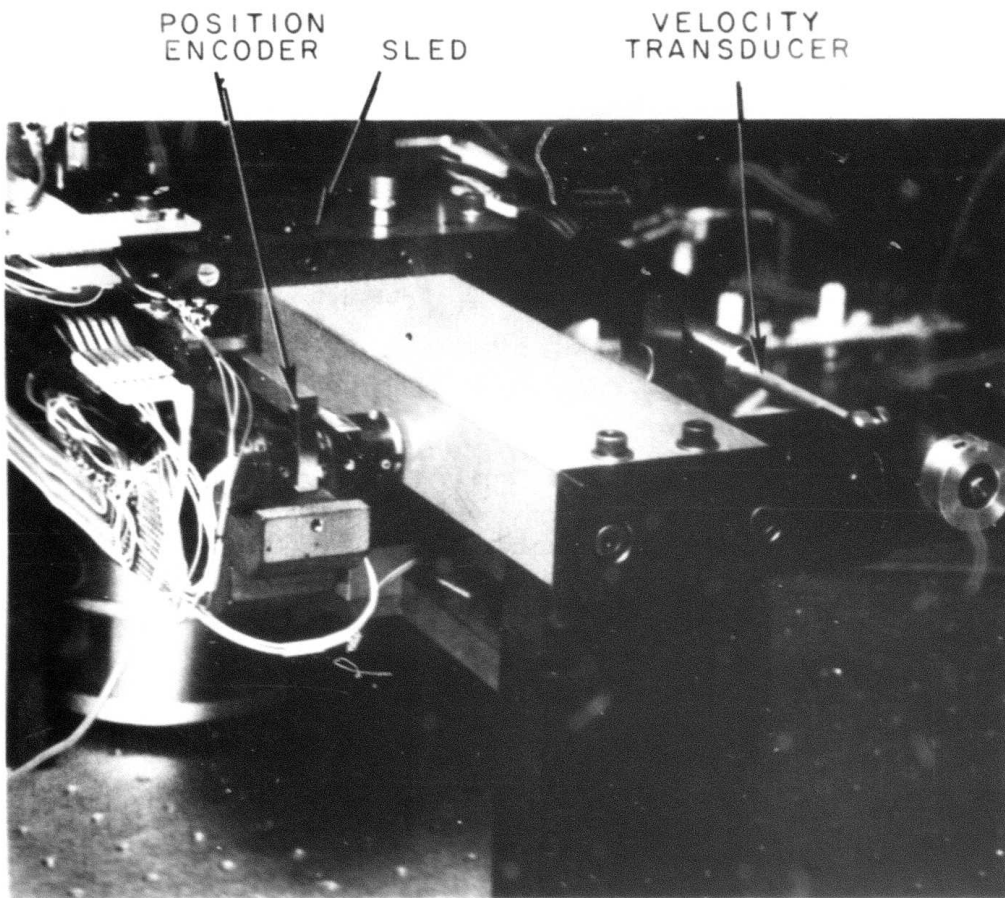


Figure 36: Fast access sled.

## 10. COMPARISON WITH MAGNETIC STORAGE

A comparison between the best commercially available magnetic
storage devices and the optical disc is given in Table 3.
It is not claimed that the optical disc can replace magnetic
storage media. In many applications where erasure is necessary,
the optical disc is unsuitable. However, optical recording does
offer some potential advantages, viz., a low-cost and efficient
storage medium, and improved archival properties. The media
cost is estimated at $5 \times 10^{-8}$ cent/bit; the hardware cost is
estimated at $5 \times 10^{-5}$ cent/bit. The volumetric storage effi-
ciency of the optical disc is 48 times better than 6250 bpi mag-
netic tape. The cost and size advantages are primarily due to the
very high storage density of optical recording ($2 \times 10^8$ bits/in$^2$).

## 11. CONCLUSIONS

The major accomplishment of this program was the design, fabri-
cation and test of a direct read after write (DRAW) optical disc
recorder system. The choice of tellurium as a recording medium
allows direct monitoring of the recording quality; no development
or fixing of the recording is necessary. The selection of a
PMMA master disc yields considerable cost and storage benefits
as compared to a polished glass master. The air-sandwich
protective mechanism localizes the "clean room" requirement to
the disc itself, thereby eliminating the special handling
precautions that unprotected glass masters would require and
eliminating the need for a Class 100 clean room. The system
could be produced in large quantities at or near the target
prices. In summary, all of the program goals were met by
accomplishment of these key tasks:

- Design, fabrication, and test of a prototype DRAW recorder.
- Selection of a suitable disc substrate (Plexiglas).
- Design and test of a disc protective mechanism (air sandwich).
- Demonstration of two suitable DRAW materials
  (tellurium and bismuth).
- Shelf-life characterization of tellurium and bismuth.
- Demonstration of a working error-detection and
  correction system.
- System concept amenable to a disc cost of <$10 and a
  recorder cost of <$10,000 in production quantities.

TABLE 3: Characteristics of mass storage devices.

| DEVICE | CAPACITY (bits) | ACCESS TIME (ms) | DATA RATE (Mbit/sec) | HARDWARE COST | MEDIA COST ($) | COST/BIT (cents) | ARCHIVAL LIFE |
|---|---|---|---|---|---|---|---|
| Magnetic Disc[3] IBM 3340 | $5.5 \times 10^8$ | 35 | 7.0 | $20,000 | $2,200 disc pack | $4 \times 10^{-4}$ | 2-3 yrs? |
| 6250 B.P.I. Tape IBM 3420 | $7.4 \times 10^8$ | 60,000 | 3.7 | $30,600 | $16.50 2400' reel | $2.2 \times 10^{-6}$ | 1-2 yrs. |
| Mass Storage System IBM 3850 | $3.7 \times 10^{12}$ | 16,000 | 7 | $2,400,000 | $188,000 9400 cartridges @ $20 ea. | $5 \times 10^{-6}$ | 1-2 yrs. |
| Philips Labs Optical Disc | $2 \times 10^{10}$ | 100 to 500 | 2-10 | $10,000 | $10 | $5 \times 10^{-8}$ | >10 yrs. |
| Philips Labs Optical Disc Pack | $10^{12}$ | 50 to 100 | 20-50 | $200,000 | $150 | $1.5 \times 10^{-8}$ | >10 yrs. |

Notes: 1. Performance and costs of IBM equipment from "DATAPRO".

2. Performance and costs of Optical Disc Equipment are best estimates only.

3. Largest drive with removable disc pack.

## 12.     FUTURE CONSIDERATIONS

The Philips/MCA consumer videodisc system maps about 6 bits of information to each pit on the disc.  The recording format chosen for the digital disc conservatively assigns only one bit to a recorded pit.  This format choice results in very high noise margins which could be later traded for increased recording densities.  Future research and development in optical recording will involve increasing the storage capacity of the disc to about $10^{11}$ bits.  Techniques to be investigated are:  smaller track spacing, more efficient data encoding, and increasing the number of encoded bits per recorded pit.  Additionally the trade-offs between cost, laser power, and speed will be explored at data rates of at least 50 Mbit/s.  Reduction of access times to the tens of ms range is also possible using the technology developed for magnetic disc drives.

A system using an optical disc pack of 6 double-sided discs, accessed by 12 separate optical read heads, could be considered (Table 3).  Each disc pack would have a storage capacity of $10^{12}$ bits, and each of the 12 disc surfaces would be accessed by its own optical head for recording and playback.  Such a disc pack would represent the first known _portable_ storage device for one trillion bits.  At an estimated volume price of $150 each, the cost per bit ($1.5 \times 10^{-8}$¢) is even less than a photograph (Ref. 15).

Figure 37 shows the design for a disc pack with 6 double-sided discs and one of the optical heads.  The disc pack size is 45.5 cm x 9 cm (17.9" x 3.5"); this is about the same size (volume) as an IBM 2316 disc pack.  The spacing between the discs would be determined by the minimum size of the optical head.

A "jukebox" arrangement of 1000 disc packs could expand the on-line system capacity to $10^{15}$ bits.  Such a system would be as equivalent in capacity and cost ($\approx$\$2.5m) as the IBM 3850

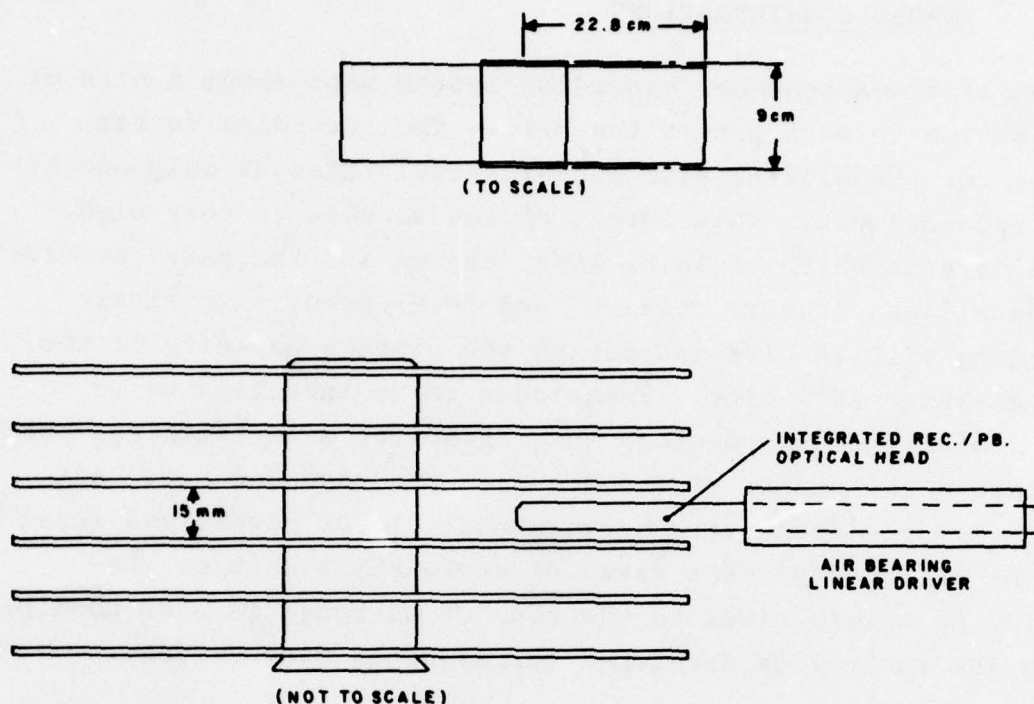Figure 37: Design of optical disc pack with six
double-sided discs.

mass storage system. The access time (16 sec) and space require-
ments would also be similar.

If quick access is not important, then the basic optical disc
pack system ($200,000) could be expanded to $10^{15}$ by simply
storing 1000 disc packs in a 325 square foot room. The media
cost for $10^{15}$ bits would be only $150,000.

13.　　　REFERENCES

1.　　P. W. Bogels, "System Coding Parameters, Mechanics and Electro-Mechanics of the Reflective Videodisc Player", IEEE Trans. Consumer Elect., Nov. 1976.

2.　　D. Maydan, "Micromachining and Image Recording on Thin Films by Laser Beams", Bell System Tech. Journal, July-Aug 1971.

3.　　C. Becker, H. Dell, "Laser Recording Medium", U.S. Patent No. 3,665,483.

4.　　J.S. Winslow, "Mastering and Replication of Reflective Videodisc", IEEE Trans. Consumer Elect., Nov. 1976.

5.　　App. II of Philips Laboratories Qtly. Tech. Report, "Development of an Optical Disc Recorder", April-June 1976, DARPA Contract No. N00014-76-C-0441.

6.　　App. B of Philips Laboratories Qtly. Tech. Report, "Development of an Optical Disc Recorder", July-Sept 1976, DARPA Contract No. N00014-76-C-0441.

7.　　App. C of Philips Laboratories Qtly. Tech. Report, "Development of an Optical Disc Recorder", July-Sept 1976, DARPA Contract No. N00014-76-C-0441.

8.　　App. B of Philips Laboratories Qtly. Tech. Report, "Development of an Optical Disc Recorder", Oct- Dec 1976, DARPA Contract No. N00014-76-C-0441.

9.　　App. C of Philips Laboratories Qtly. Tech. Report, "Development of an Optical Disc Recorder", Oct-Dec 1975, DARPA Contract No. N00014-76-C-0441.

10.　App. I and II of Philips Laboratories Qtly. Tech. Report, "Development of an Optical Disc Recorder", Jan-Mar 1976, DARPA Contract No. N00014-76-C-0441.

11.　J.C. Mallinson and J.W. Miller, "Optimal Codes for Digital Magnetic Recording", The Radio and Electronic Engineer, Vol. 47, No. 4, pp 172-176, April 1977.

12.　J.A. Heller, "Feedback Decoding of Convolutional Codes", Advances in Communication Systems, Vol. 4, Academic Press Inc., 1975.

13.　Linkabit Corp. "Instruction Manual LF1011-256 Convolutional Encoder Feedback Decoder", San Diego, Calif. 92121, 1973.

14.　App. A of Philips Laboratories Qtly. Tech. Report, "Development of an Optical Disc Recorder", Jan-Mar 1977, DARPA Contract No. N00014-76-C-0441.

15.　L. Roberts and B. Wessler, "Computer Network Development to Achieve Resource Sharing", Proc. 1971 SJCC, AFIPS Conf. Proc., Atlantic City, N.J.

APPENDIX A


TEMPERATURE STRESS AGING OF OPTICAL DISC
RECORD MEDIA

by

Alfred Milch
Pedro Tasaico

# TEMPERATURE STRESS AGING OF OPTICAL DISC
## RECORD MEDIA

by

Alfred Milch
Pedro Tasaico

## 1.  INTRODUCTION

The archival value of an optical disc record is largely deter-
mined by the long time stability of the medium under environ-
mental stress.  An important component of this stress is tempera-
ture.  Tests were performed at several temperatures for a period
of about fourteen months.

For testing, small (18 mm square) samples of polymer were cut,
cleaned according to a standard procedure and coated via vacuum
evaporation with light absorbing films.  Nominal thicknesses
were 300 Å for tellurium and 500 Å for bismuth.  The several
potential recording media tested are listed in Table I.

TABLE I:  Polymer-film combinations
tested for environmental stabililty

| Polymer | Supplier | Film |
|---------|----------|------|
| PMMA[1] | Electroglas | Te, Bi |
| PMMA | Rohm | Te |
| PVC[2] | AIN Plastics | Te, Bi |
| PVC/PVAc[3] | Polygram | Te |
| PC[4] | Westlake Plastics | Te, Bi |
| Glass | Corning (micro-scope cover slip) | Te, Bi |

_____

(1)  Polymethylmethacrylate
(2)  Polyvinylchloride
(3)  Polyvinylchloride/polyvinyl acetate
(4)  Polycarbonate

In testing, the properties that were followed as a function of aging were gross changes in the appearance of the films, the sensitivity of the films to hole formation by laser machining, and optical transmission and reflection. There were no obvious changes in transmission and reflection as a function of aging, and most changes in general appearance were attributed to the effects of handling.

## 2.   EXPERIMENTAL APPROACH

The best indicator of aging was found to be changes in sensitivity as a function of time. In fact, as the testing time lengthened, differences in sensitivity as a function of temperature began to appear. It therefore became possible to predict shelf life by employing the Arrhenius equation assuming that a first order rate governs the change in hole forming efficiency:

$$R \doteq k' = Ae^{-E_a/kT} \tag{1}$$

where,  $k'$ = reaction rate constant

$R$ = reaction rate ($\sim k'$ for first order reaction)

$A$ = constant

$E_a$ = activation energy

$k$ = Boltzmann constant ($8.617 \times 10^{-5}$ eV/deg)

$T$ = absolute temperature.

Accelerated rates or reaction times (t) at elevated temperature ($T_{acc}$), and at the normal storage temperature ($T_{st}$) may be compared via equation 1 as follows:

$$\frac{R_{acc}}{R_{st}} = \frac{t_{st}}{t_{acc}} = \exp\left[\frac{E_a}{k}\left(\frac{1}{F_{st}} - \frac{1}{T_{acc}}\right)\right] \tag{2}$$

76

where the first equality implies equal chemical action at each temperature. The ratio $t_{st}/t_{acc}$ is the acceleration factor and defines the time at normal storage temperature required to produce the same degradation observed at the high temperature. The stress aging test temperatures employed in this work were 55°C, 75°C and 90°C. Accordingly, the acceleration factor is plotted vs. $E_a$ with these temperatures as the parameter in Figure A1. Predicted life at 25°C may be obtained from this figure by multiplying time under test by the acceleration factor corresponding to the appropriate activation energy and test temperature.
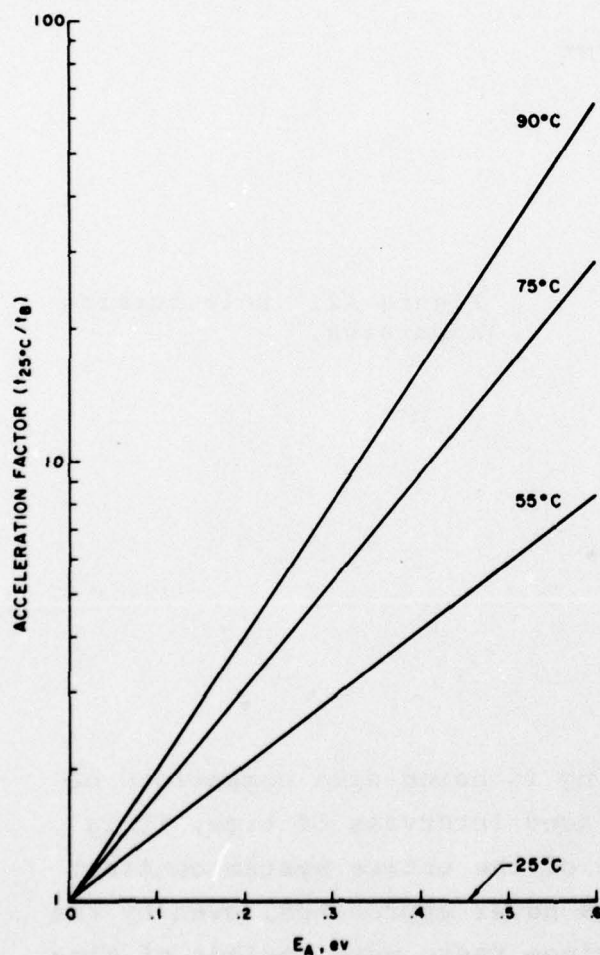


Figure A1: Accelerated aging function.

## 3.     APPARATUS AND METHOD

The apparatus for producing holes is shown in Figure A2.  It
consists of three major parts:  an argon laser (emitting at
4881 Å), the modulator, and the focussing arrangement.  The
main operational variables of this system are laser power
output, optical alignment, transmission efficiency, beam spot
size and shape at focus, extinction ratio of the modulator and
pulse shape.  Desirable operating conditions are constant power
density at focus, high extinction ratio in the modulator, a
square pulse, and a focussed spot that is circular, has a
Gaussian energy distribution, and is about one micron in
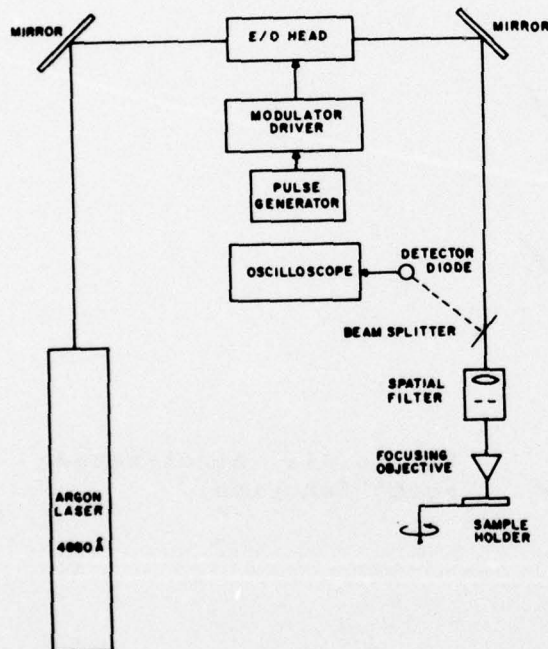diameter.  The hole size of interest is one micron in diameter.



Figure A2:  Hole forming
apparatus.

Since the concept of life testing is based upon comparison of
results obtained over widely spaced intervals of time, it is
crucial to hold the performance of the entire system constant
in every aspect.  This ideal was never approached, even by the
most painstaking maintenance, since there were periods of time
during which the equipment was disabled for purposes unrelated
to this work.

The system was operated in the out-of-focus, static mode, which allowed large numbers of observations to be made in a relatively short time. The beam is incident on the film side on the sample. A sample is caused to pass through the pulsed laser beam several times at different beam power levels. In this way, tracks of laser produced holes of different sizes are impressed on the metal films. For each track, the largest hole corresponds to the best matching between beam power level, out-of-focus spot size, pulse duration and the thermal properties of the metal film-substrate. The samples are later photographed at 400X and 2000X magnification in order to record and measure the resulting tracks. Typical examples are shown in Figure A3. A disadvantage of this method is that the large holes are formed by laser beams whose degree of focus and hence energy distributions change from moment to moment as the sample traverses the beam. Thus, while the total power which forms the hole is known, the energy distribution is not. In particular, that portion of the out-of-focus beam which is effective in hole formation is unknown. Nevertheless the ratio of total beam power to hole area is known, and this constitutes an upper limit on the power required to form the hole. Moreover, as the laser power is reduced, the formed holes decrease in size. Eventually the condition is reached where the largest hole is provided by the in-focus beam. This is simultaneously the point of greatest interest and the point at which the out of focus error is minimized. In practice, a considerable degree of subjectiveness is introduced by the necessity for choosing "largest" holes from sets of images on relatively grainy high speed film. Every effort was made to counter this difficulty statistically by obtaining large amount of data over a wide range of hole sizes.

A hole forming experiment comprises the measurement of a 2000X photographic image diameter, D (mm), of the largest hole produced by a laser burst of known power, P (mW), and duration, $\tau$ (ns). The hole forming efficiency in $mJ/cm^2$ is defined as:

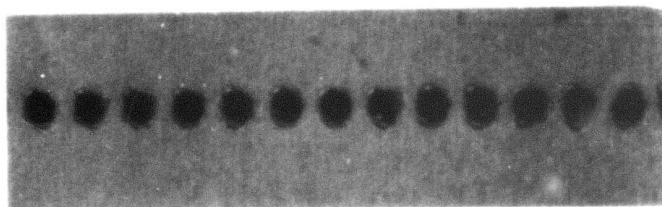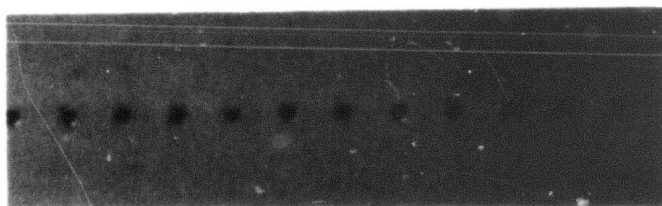$$S = \frac{P\tau \times 10^{-9}}{A} \qquad (3)$$

79

Specimen E53C
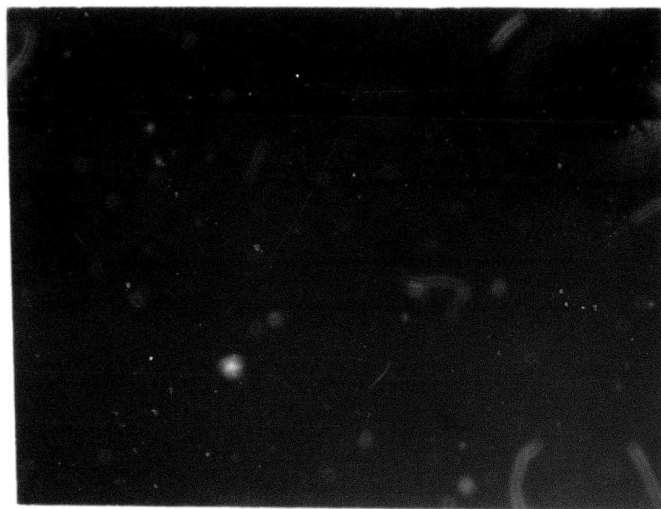
| Track # | Power mW | Hole Dia. μm | S mJ/cm$^2$ |
|---|---|---|---|
| C.W. | – | – | – |
| 1 | 12.5 | 2.6 | 177 |
| 2 | 6.7 | 1.3 | 351 |
| 3 | 5.0 | 1.1 | 361 |
| 4 | 4.0 | 1.0 | 382 |
| 5 | 3.1 | 0.6 | 701 |

400X     | 50 μm |

(a) Family portraits.

Track #1

Track #4

2000X     | 10 μm |

(b) Single tracks.

Figure A3: Static hole formations in Te on PMMA (typical).
($\lambda$ = 4881 Å, pulsewidth = 750 ns, pulse separation = 100 μs).

80

where A is the area of the formed hole.   Pulse durations are 750 ns for tellurium and 500 ns for bismuth.   In terms of the known quantities, then:

$$S_{Te} = \frac{12}{\pi} \frac{P}{D^2} \qquad\qquad (4a)$$

$$S_{Bi} = \frac{8}{\pi} \frac{P}{D^2} \qquad\qquad (4b)$$

Hole diameter is measured visually through  a 10 power loupe equipped with a graticule divided into 0.2 mm divisions Estimating to 1/2 division will result in an uncertainty in a measured linear dimension of $\pm$ 0.1/2000X (mag.) or 0.05 $\mu$m. A larger error resides in defining the photographic image hole edge.   This is typically 0.2 mm.   The net linear error of $\pm$ 0.5 mm (two edges) translates into an uncertainty of about 50% in area for a one micron hole (2 mm image).   The importance of statistically averaging large amounts of data becomes all the more obvious.

## 4.    ANALYSIS OF RESULTS

Results of one set of experiments are plotted in terms of sensitivity vs. relative hole area in Figure A4.   These graphs reveal certain important properties of the hole forming process. Firstly, and obviously, negative hole areas and S values are excluded.   Secondly, vertical and horizontal asymptotes appear. Thirdly, the vertical asymptote implies that starting a hole is very costly in energy.   Fourthly, at large hole areas, S tends toward a constant non-zero value.   Finally, the existence of the non-zero horizontal asymptote, $S_\infty$, implies that the formation of large holes depends only on the amount of material removed. Hence, $S_\infty$ should contain significant information about the thermal properties of the recording medium.
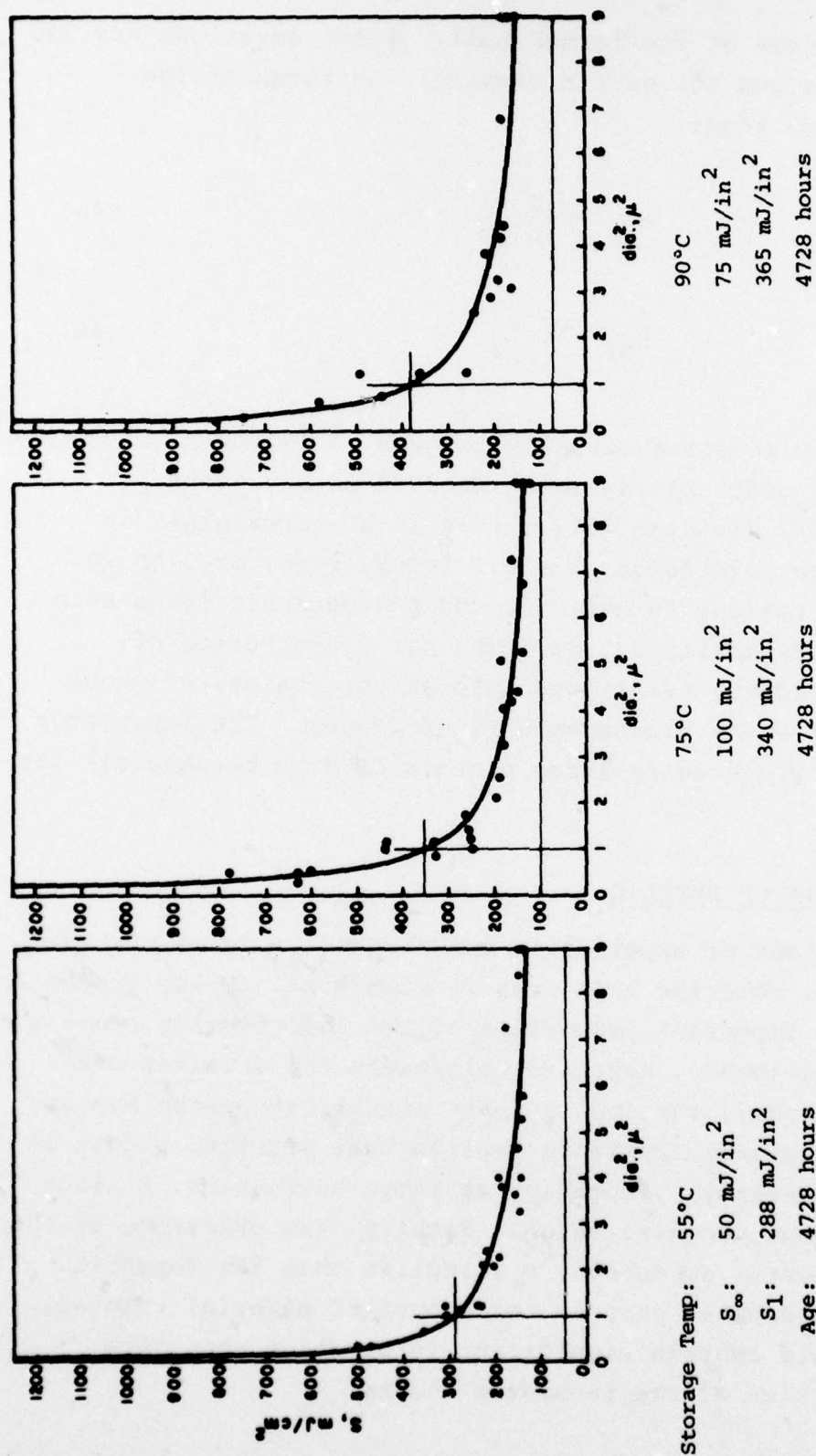
Figure A4: Hole forming sensitivity as a function of relative hole area for various accelerated aging temperatures (E38–E41, E43–E46; Te on Glasflex brand PMMA).

A statistical estimate of the sensitivity for 1 $\mu$m hole forma-
tion is arrived at by assuming a hyperbolic function of the form:

$$(S-S_\infty) \cdot d^2 = S_1 \qquad (4)$$

where the constant $S_1$, is the sensitivity for 1 $\mu$m holes.

Linearizing,

$$\ln(S-S_\infty) = m \ln d^2 + \ln S_1 \qquad (5)$$

where the slope, m, is included for generality. Equation 5 was
treated by a least squares analysis for the case in which errors
were expected in both S and $d^2$. This yielded values for m, c,
and the correlation coefficient, r. The value of $r^2$ tends
towards unity for maximum correlation between S and $d^2$. It is
a simple matter to apply the method repeatedly to a given set of
data, varying the value of $S_\infty$ as an adjustable parameter, until
$r^2$ is maximized. The lines drawn and the data presented in
Figure A4 are a result of this type of analysis.

Tellurium (300 Å thick films) on PMMA was studied most exhaus-
tively. Thirty-eight samples were followed for over 10,000
hours, during which time over 600 pairs of S vs. hole diameter
measurements were made. The results are gathered in Table II.

A least squares analysis was applied to these data assuming a
constant rate of change, R, of $S^{(*)}$ as a function of time:

$$S = S_0 + Rt \qquad (6)$$

assuming no errors in the time axis. The method yielded, in
addition to the slope and intercept, the one-standard-deviation
errors on the slope $\varepsilon_r$ and intercept $\varepsilon_b$, and the standard
deviation of the fit, $\sigma$. These results are shown in Table III.

---

* For simplicity, the subscript "1" denoting sensitivity for
  1 $\mu$m holes is omitted.

83

## TABLE II: Sensitivity for formation of
## 1 $\mu$m holes in 300 Å Te films on PMMA

| Age Thousands of Hours | Temperature 328°K | Temperature 348°K | Temperature 363°K | Experiment I.D. and Brand of PMMA |
|---|---|---|---|---|
| | $mJ/cm^2$ | $mJ/cm^2$ | $mJ/cm^2$ | |
| 0 | 416 | 348 | 396 | E38-41,E43-46 |
| 1.00 | 345 | 362 | 352 | sixteen samples; |
| 1.90 | 320 | 358 | 332 | Glasflex brand |
| 2.90 | 311 | 385 | 337 | |
| 4.73 | 288 | 340 | 365 | |
| 8.90 | 408 | 435 | 510 | |
| 0 | 308 | 326 | 283 | E31, six samples; |
| 0.36 | 360 | 350 | 306 | Glasflex brand |
| 1.66 | 328 | 270 | 325 | |
| 3.22 | 362 | 289 | 552 | |
| 10.20 | 482 | 456 | 517 | |
| 0 | 417 | 424 | 428 | E49-E56 sixteen |
| 0.96 | 365 | 383 | 321 | samples; Rohm |
| 5.52 | 412 | 477 | 454 | brand |

## TABLE III: Decay rates for 1 $\mu$m hole formation
## in Te on PMMA as a function of temperature

| | Temperature 328°K | Temperature 348°K | Temperature 363°K |
|---|---|---|---|
| $r(\Delta S/1000\ hrs) + \varepsilon_r$ | 7.8 $\pm$ 4.2 | 10.0 $\pm$ 4.4 | 18.1 $\pm$ 5.6 |
| $S_o \pm \varepsilon_b$ | 343 $\pm$ 14 | 342 $\pm$ 14 | 338 $\pm$ 18 |
| Standard deviation of fit, $\sigma$ | 50 | 53 | 67 |

The one-standard-deviation error envelope for predicting the
location of the line within a confidence interval of 50% is
given by:

$$\varepsilon_{line} = \pm\sqrt{\varepsilon_b^2 + \varepsilon_r^2 t^2} \qquad (7)$$

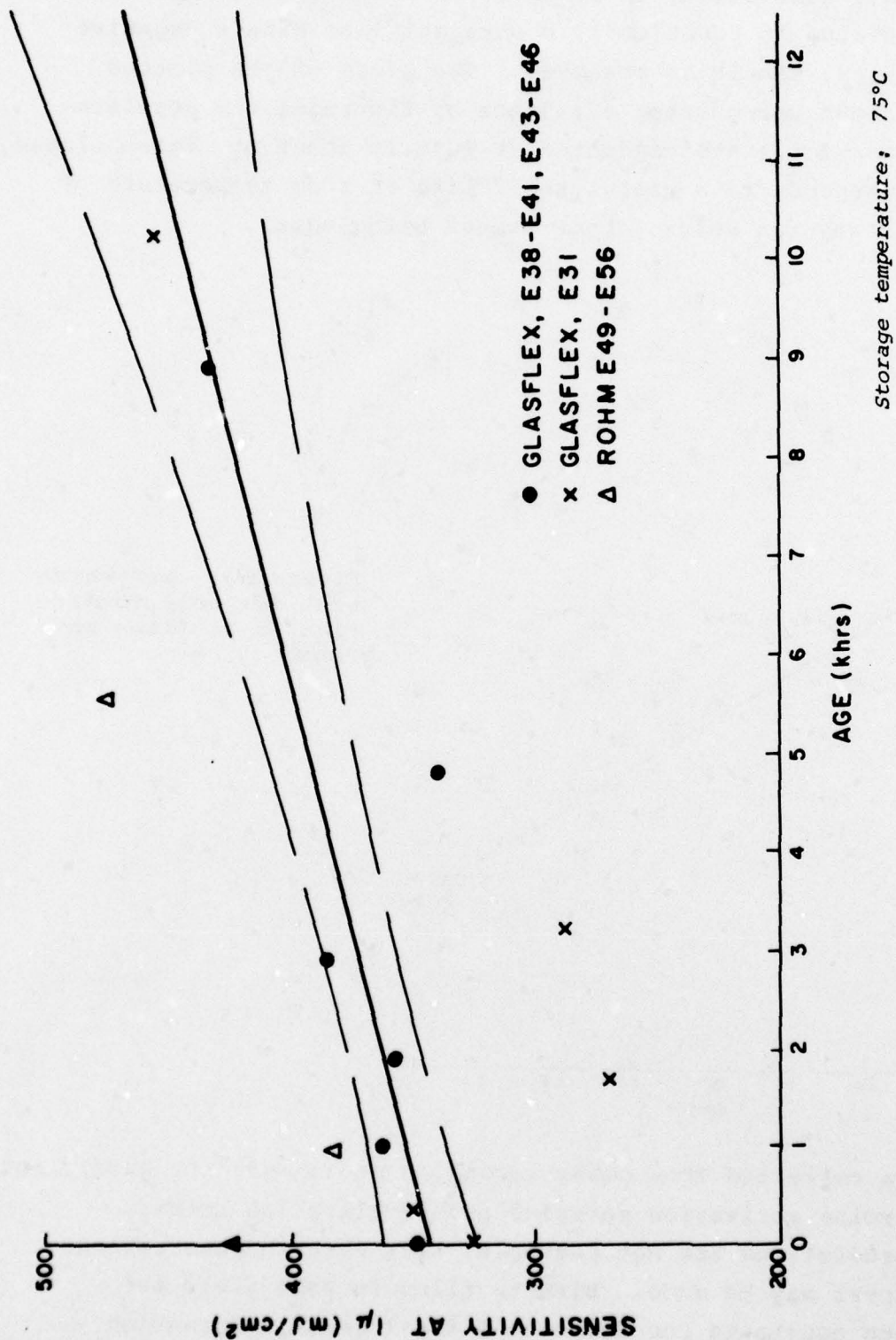Equations 6 and 7 are plotted in Figure A5 for a typical case.

Figure A5: Typical aging characteristic of Te on PMMA with respect to hole formation.

The temperature dependence of the rate of change of the one micron hole sensitivity is shown in an Arrhenius plot in Figure A6. According to Equation 1, a straight line with a negative slope ($-E_a/k$) should be observed. The slope of the plotted line is about one-quarter eV; hence by Figure A1 the acceleration factor for tests conducted at 90°C is about 6. Extrapolated, this corresponds to a useful shelf life at room temperature of approximately ten years, other things being equal.
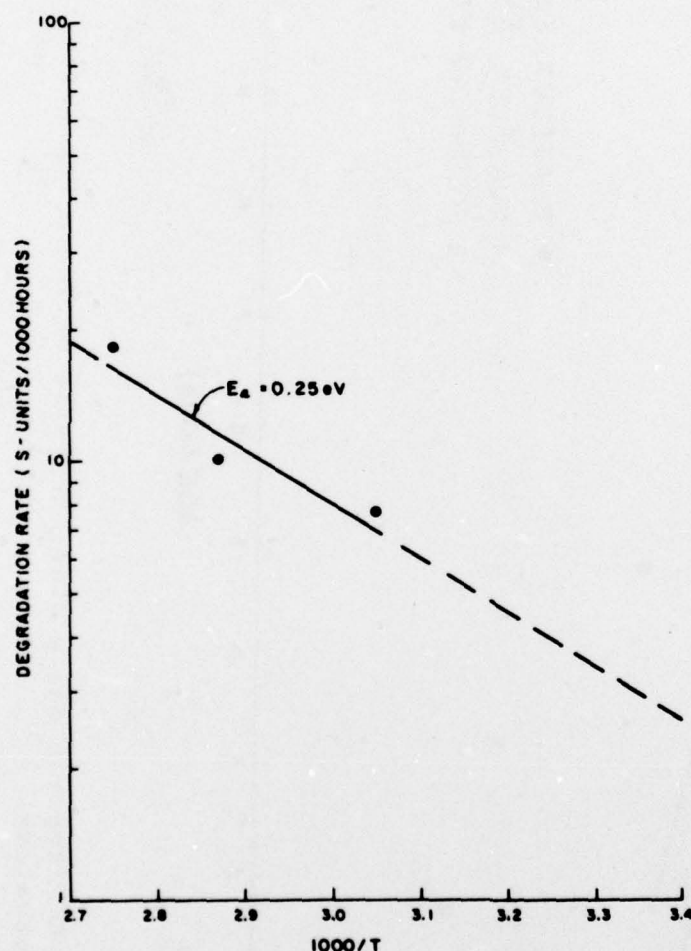


Figure A6: Arrhenius plot for hole formation in Te films on PMMA.

The data collected from other recording media were not sufficient to determine activation energies and acceleration rates; hence predictions are not possible. Yet certain observations of interest may be made. Bismuth films on PMMA yield the following constants for Equation 6 for 1 $\mu$m hole formation (lumped data from several runs at various temperatures):

Rate r in S-units/1000 hours:  -21

Intercept, $S_o$ in mJ/cm$^2$       :   617

The bismuth films appear to improve with time over one year;
hence, the significance of a change in S after one year is
unclear.  Preliminary observations for new films on polycarbonate
are:

| Film | S |
|------|---|
| Bi | 754 mJ/cm$^2$ |
| Te | 336 mJ/cm$^2$ |

During the work on tellurium, optical reflection and transmission
were measured.  There were no discernable temperature effects
over the temperature range investigated.  Therefore, data for
all temperatures were lumped.  The results are displayed graph-
ically in Figure A7.  The linear least-squares lines are drawn in
Figure A7, and the corresponding derived parameters are tabulated
below.

TABLE IV:  Optical properties of 300 Å
Te films on PMMA (Runs E38-E41, E43-E46)

| | Transmission parts per thousand | Reflection percent | Absorption percent |
|---|---|---|---|
| Slope | +0.49 ± 0.48 | −0.23 ± 0.21 | +0.14 ± 0.21 |
| Intercept | 25 ± 2 | 52 ± 1 | 46 ± 1 |
| Standard deviation of fit, σ | 4 | 2 | 2 |

The available data and the derived least-squares parameters
indicate that within the experimental error the optical properties
of these films did not change over the course of one year.  The
absence of measureable changes precludes the establishment of an
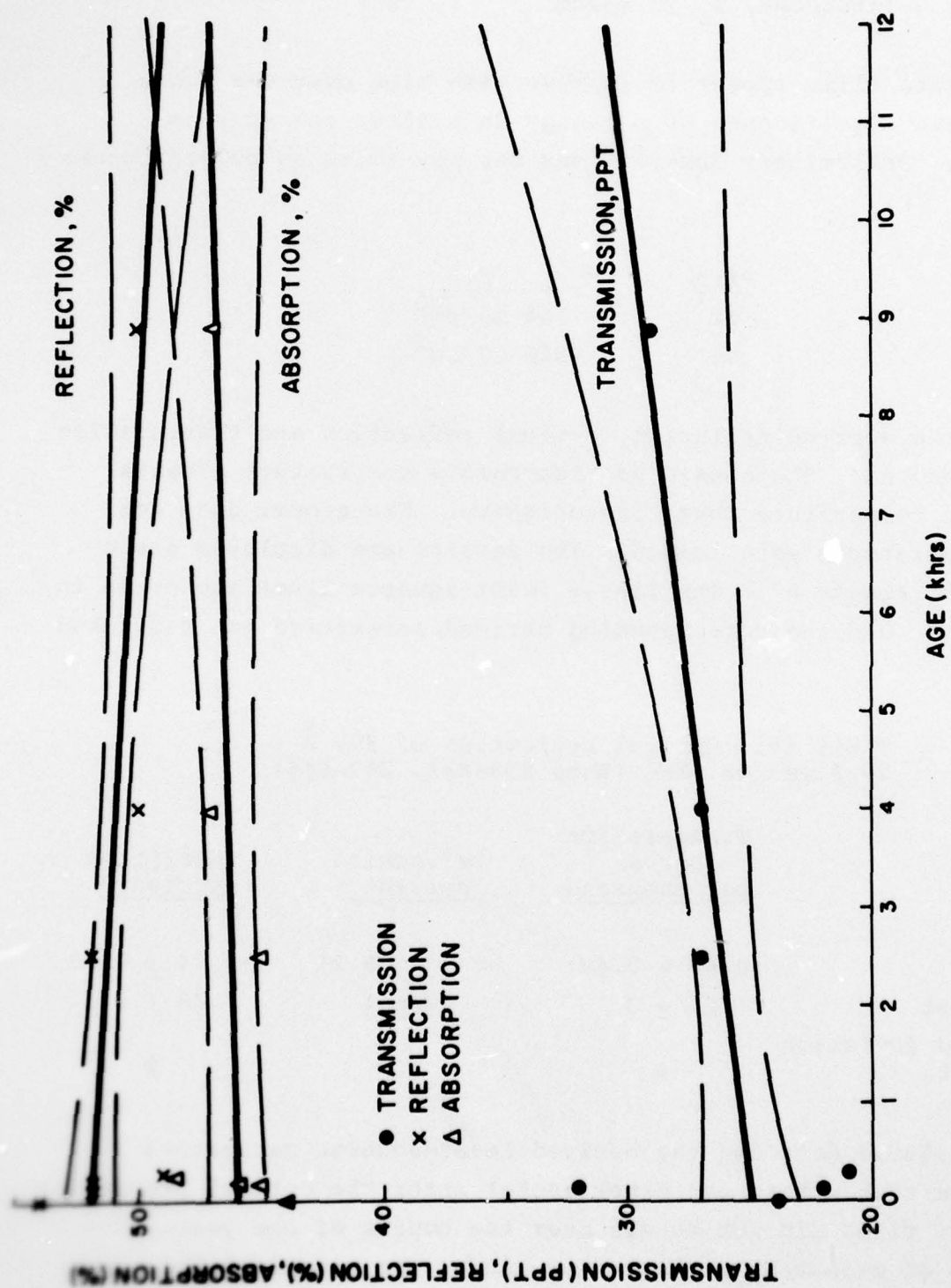activation energy for any of these optical properties,

Figure A7: Optical properties of Te films on PMMA as a function of age (all temperatures).

hence extrapolations to longer times are difficult. If normal oxidative processes are presumed responsible for what changes there are, then it may be plausible to assume that the film/substrate combinations will retain their optical properties for a *decade or more.*

## 5. <u>CONCLUSIONS</u>

From all of the above, tellurium seems to be the film material of choice. Of the plastic substrates, Glaslfex brand PMMA appears to be the most stable of all.

**APPENDIX B**

**TURNTABLE WITH PHASE LOCKED SPEED CONTROL**

by

Robert McFarlane

<div align="center">

TURNTABLE WITH PHASE LOCKED SPEED CONTROL

by

Robert McFarlane

</div>

## 1.     INTRODUCTION

This note describes the design and performance highlights of a
precision turntable servo for optical disc recording.  The
turntable is a low-friction, high-inertia device consisting of
an air bearing (Professional Instruments Co. Model 4B Blockhead),
a printed circuit dc motor (PMI Model U9M4) with an optical
shaft angle encoder having 2000 cycles per revolution.  The only
significant contribution to friction comes from the motor brush
contact.

The air bearing provides a precise shaft position for the
optical disc with runout less than 1 $\mu$m.  However, the high
inertia of the air bearing limits the attainable acceleration of
the particular motor-bearing combination.

Speed control is attained by building a phase locked loop around
the motor using a crystal-derived reference frequency.  Phase
lock is established by phase comparison of the reference fre-
quency and the frequency generated by the optical shaft-angle
encoder.

## 2.     SYSTEM DESCRIPTION

A block diagram of the phase-locked motor servo is shown in
Figure B1.  A crystal-derived reference frequency is phase
compared with a frequency generated by an optical encoder
attached to the motor shaft.  The error signal, which is pro-
portional to the phase difference of the two frequencies, is
used to power to motor.  This section describes the derivation
of the open loop transfer function and the schematic repre-
sentation of the electronics.
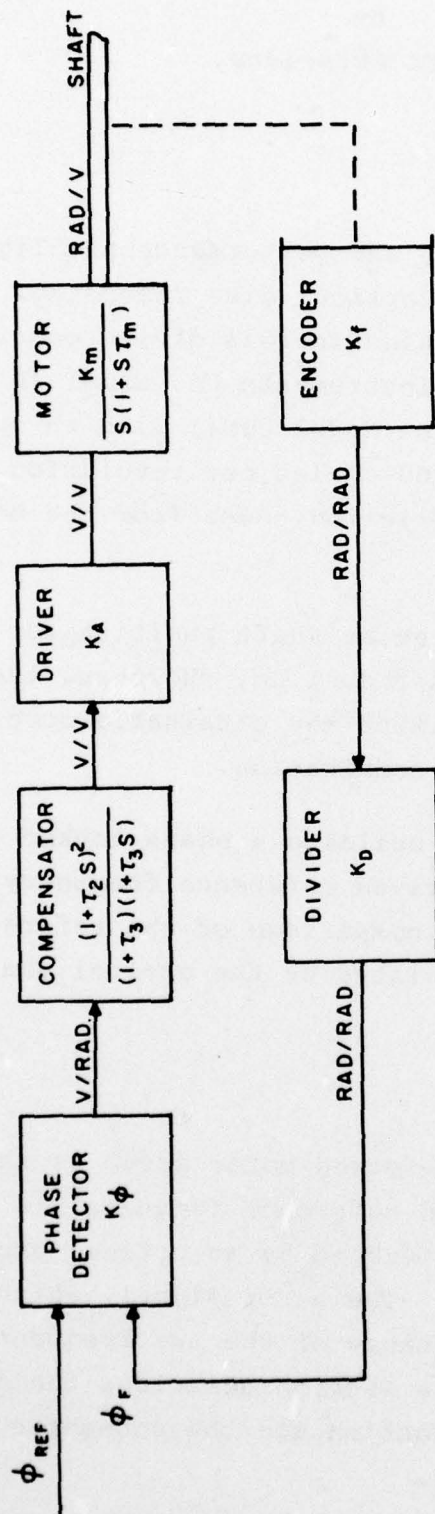
OPEN LOOP TRANSFER FUNCTION = $K_\phi\, K_A\, K_m\, K_f\, K_D \dfrac{(1+\tau_2 S)^2}{S(1+\tau_1 S)(1+\tau_3 S)(1+\tau_m S)}$

Figure B1: Block diagram of turntable servo.

The transfer function of the motor is:

$$\frac{\phi(s)}{V(s)} = \frac{1/K_e}{s(1+s\ \tau_m)}\ \text{rad}$$

where, $\phi(s)$ = angular displacement, $V(s)$ = applied voltage, $K_e$ = emf constant of the motor, and $\tau_m$ = mechanical time constant of the motor and load. The manufacturer's specification for the Model U9M4 motor gives $K_e$ = 5.0 V/1000 rpm from which is derived $K_m$ = 21 rad/V at unity angular frequency.

The mechanical time constant is given by the expression:

$$\tau_m = R_m J$$

where, $R_m$ = motor regulation at constant voltage, and J = total moment inertia at the shaft. For the U9M4 motor $R_m$ = 4.66 x $10^3$ rpm/m$^2$kg s$^{-2}$ (rpm/N-m).

The total moment of inertia is the sum of contributions from the air bearing, disc, and motor rotor, the last of which may be neglected. The inertia of the air bearing is 2.82 x $10^{-3}$ kg/m$^2$ and that of a plastic air sandwich 0.08 in. thick is 1.89 x $10^{-3}$ k/gm$^2$ so that the mechanical time constant is:

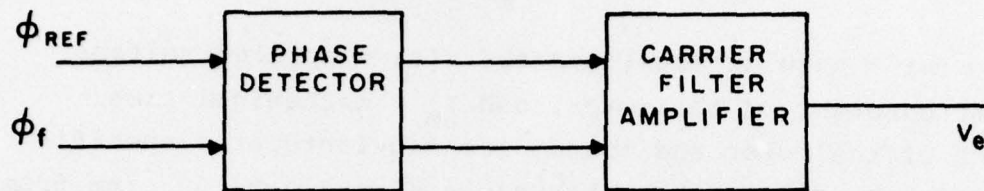$$\tau_m = 4.66\ \text{x}\ 10^3\ \text{rpm/m}^2\ \text{kg}\ \text{s}^{-2}\ \text{x}\ 4.71\ \text{x}\ 10^{-3}\ \text{k/gm}^2 = 2.3\ \text{s}$$
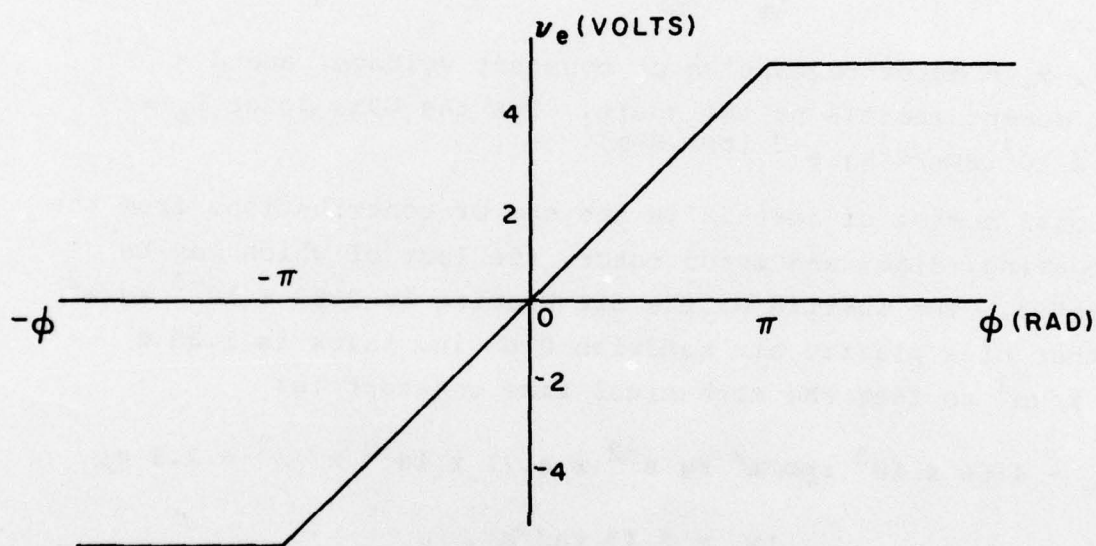
$$(w_m = 0.43\ \text{rad/s}).$$

Figure B2 shows the block diagram and transfer characteristic of the phase detector. The value of $K_p$ is 1.75 V/rad.

The resolution of the optical shaft angle encoder is 2000 cycles per revolution (rad/rad), and the frequency is divided by ten before entering the phase detector ($K_d$ = 0.1). The driver $K_a$ is unity.

The open loop transfer function of the system without compensation becomes:

Figure B2:  Phase detector.

$$GH(s) = \frac{7350}{s(1+2.3s)}$$

Because of the large mechanical time constant, the system bandwidth with compensation is limited to about 50 rad/s (as shown in Fig. B3), and the open loop transfer function becomes:

$$GH(s) \cong \frac{7350s(1+.25s)^2}{s(1+2.3s)(1+10s)(1+.005s)(1+.01s)}$$

The phase margin computed for a crossover frequency of 50 rad/s is 67.5°. Figure B4 shows the schematic of the servo amplifier. The reference frequency is derived from a 2.4 MHz crystal oscillator, and the reference frequency can be selected to provide rotational speeds of 1800 rpm, 600 rpm and 180 rpm.

3.    SPEED ERRORS

Two methods were used to measure the short term (once around) speed variation. In one method the variation of time displacement between the encoder and reference pulses at the input to the phase detector was measured. In the other, the oscilloscope was triggered on a random encoder pulse, and the time variation of the corresponding pulse after one revolution was measured. The second method was applied to the internal optical encoder and also to a contactless magnetic encoder in proximity to the turntable shaft. All the above measurements produced the same result of 1 $\mu$s error at 1800 rpm and 10 $\mu$s error at 180 rpm (0.003%).

The speed variation within one revolution is obtained from the waveform of the servo error signal. Figure B5 shows the error signal during one revolution at 1800 rpm and 180 rpm.

The instantaneous speed error is:

    Speed error =

    $\dfrac{\text{(slope of error signal)V/s (Phase det. const)rad/V}}{\text{(encoder divider const)rad/rad}(2\pi)\text{rad/rev}}$

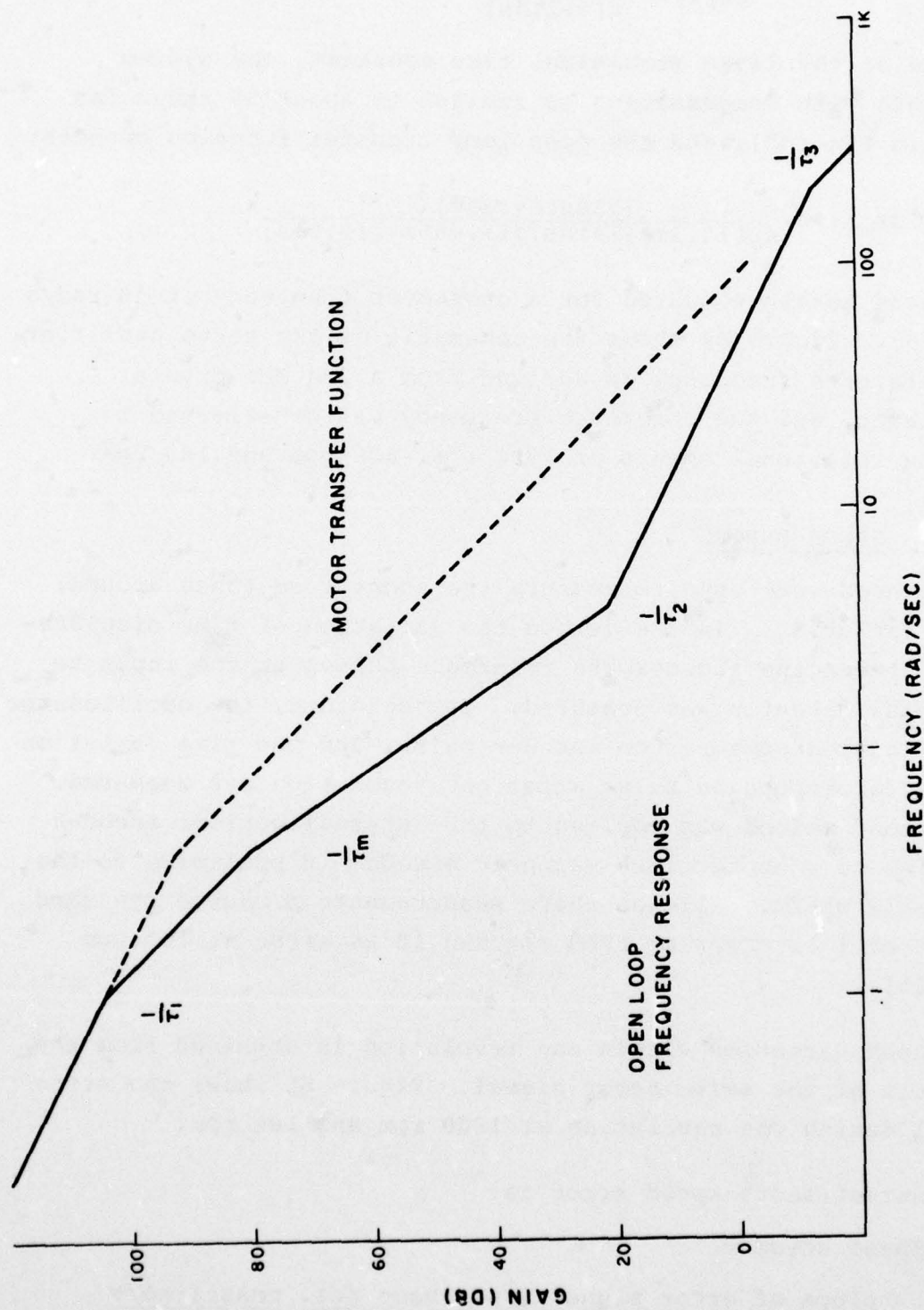where, the phase detector constant = 0.57 rad/V and the encoder
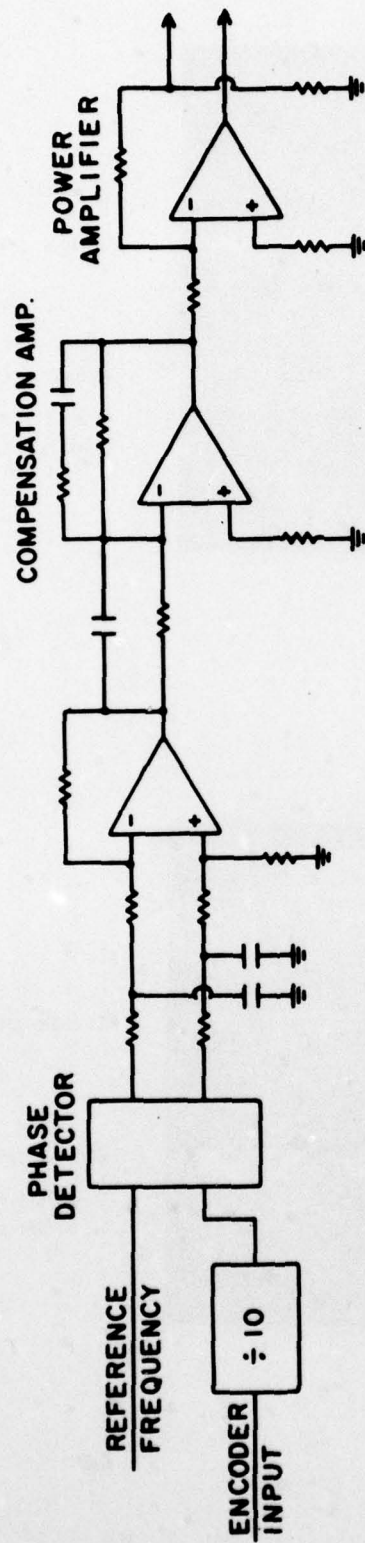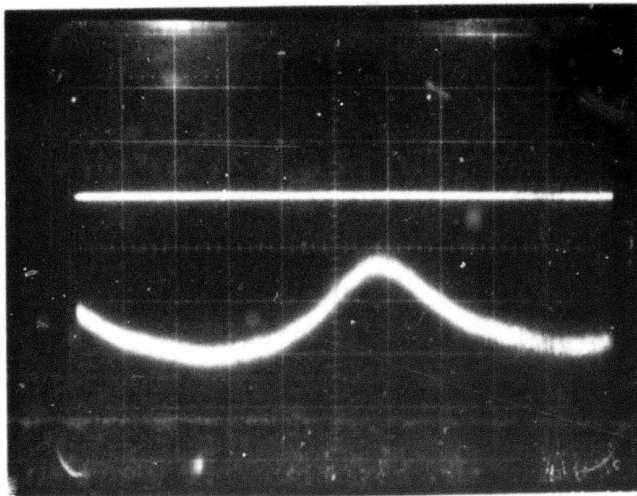
97

Figure B3: Open-loop frequency response.

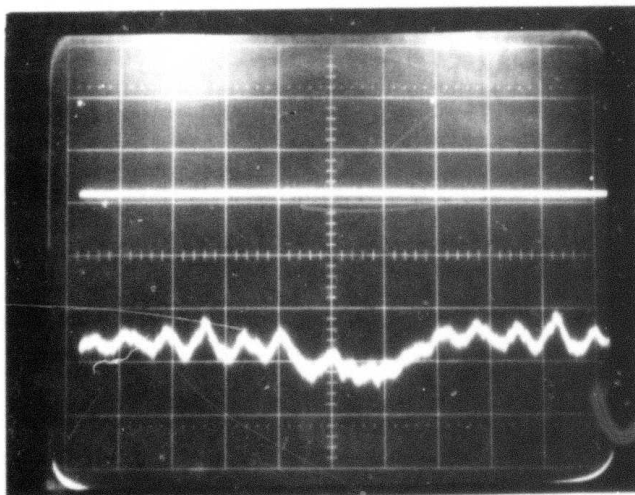Figure B4: Turntable servo amplifier.

Index pulses

Error voltage
V = 10 mV/Div.
H = 5　ms/Div.

(a)  1800 rpm



Index pulses

Error voltage
V = 10 mV/Div.
H = 50 ms/Div.

(b)  180 rpm

Figure B5:    Servo error voltages.

100

divider constant = 200 rad/rad. For operation at 1800 rpm (30 rps), the steepest slope is 1.5 V/s, and the corresponding speed error is $6.75 \times 10^{-4}$ rps (0.00225%) which is roughly equivalent to the once around error.

For operation at 180 rpm, the error voltage variation is more complex. The slower speed variation within a revolution is equivalent to that encountered at 1800 rpm (0.00225%). However, the faster speed variations at a rate of about 24 cycles per rev or 450 rad/s, produced instantaneous speed errors an order of magnitude larger, because the servo bandwidth is only 50 rad/s. These variations are due to high-frequency torque ripple which is significant at low speeds.

The long-term speed error was determined by measuring the period of the index pulse on a digital counter with a one-second sampling rate. For both speeds, 1800 rpm and 180 rpm, the long-term speed variation was one part in $3 \times 10^5$ equivalent to the tolerance of the reference crystal.

For all the above measurements, the results were the same for horizontal or vertical orientation of the turntable shaft and for the turntable unloaded or loaded with an air sandwich disc that exhibited a visible unbalance.

## 4.    CONCLUSIONS

The system described provides more than adequate speed control for digital recording. The design goal was 0.1% short term speed error.

The turntable was fabricated from readily available components. If future needs call for  better than 0.03% speed accuracy, it would be desirable to explore the possibility of obtaining suitable air bearings with lower inertia so that improvements can be made in acceleration and servo bandwidth. Improvements in this area should reduce the instantaneous speed errors especially a low operating speeds.